Chapter - 3

Synthesis and mesomorphic properties of

(i) 2,7-Naphthylene bis[4-(E-4-n-alkoxycinnamoyloxy)2-fluorobenzoates] (Series-3.I)

(ii) 2,7-Naphthylene bis[4-(E-4-n-alkoxy-α-methylcinnamoyloxy)2-fluoro-benzoates] (Series-3.II)

(iii) 2,7-Naphthylene bis[4-(E-4-n-tetradecyloxycinnamoyloxy)3-fluoro-benzoate] Compound 3.C.1

(iv) 2,7-Naphthylene bis[4-(E-4-n-alkoxy-α-methylcinnamoyloxy)3-fluorobenzoates] (Series-3.III)

(v) 2,7-Naphthylene bis[4-(E-4-n-dodecyloxy-α-methylcinnamoyloxy) benzoate] Compound 3.E.1

(vi) 1,3-Phenylene bis[4-(E-4-n-alkoxycinnamoyloxy)2-fluorobenzoates] (Series-3.IV)

(vii) 1,3-Phenylene bis[4-(E-4-n-alkoxy-α-methylcinnamoyloxy)2-fluoro-benzoates] (Series-3.V)

A brief survey of banana-shaped mesogens exhibiting B-phases and a nematic phase

The design and synthesis of banana-shaped mesogens require broadly two units: (i) a central unit, which provides the bending angle and (ii) two rod-like units with a terminal aliphatic chain which could be attached to the central unit. One of the most well studied central units has been resorcinol [20, 32, 35, 36, 42, 54, 61] and its substituted derivatives [32,67]. In addition to these, 1,3-phenylenediamine, 3-aminophenol and 2,7-dihydroxynaphthalene have also been used as central units for synthesizing bent-core compounds. Most of these compounds contain Schiff's base linking group in the side arms. However, Tschierske *et al.* [42] designed and synthesized bent-core compounds not containing any of the above central units but derived from 1,3-bis(4-hydroxyphenyl)benzene; 2,6-bis(4-hydroxyphenyl)pyridine; 2,6-bis(4-hydroxyphenyl)nitrobenzene; 1,3-bis(4-hydroxyphenylethynyl)benzene; 1-(4-hydroxyphenyl)-3-(4-hydroxyphenylethynyl)benzene etc.

Most of the compounds reported above are monomesomorphic. However, smectic A, smectic C or nematic phases have been obtained either individually or in combination with B-phases. A direct transition from a nematic to a columnar B_1 phase has been observed [42] and this is due to the fact that both nematic and B_1 phases normally appear for short chain length compounds in a homologous series. Although the nematic phase was observed in many bent-core compounds [42, 52, 95] there was no example of a direct transition from an antiferroelectric B_2 phase to a nematic phase. As we shall see later, this author reported the first example of a direct transition from the antiferroelectric B_2 phase to a nematic phase. At the same time there was another report of this type of transition [48]. This compound contains 4-chlororesorcinol as the central unit and a fluorine substitutent on the outer phenyl ring at *meta* position with respect to the n-alkoxy chains. There is an another compound in which B_2 and the nematic phases are observed but are separated by smectic A and smectic C phases [67]. In both cases [48, 67], the compounds are Schiff's bases and are derived from substituted resorcinol as the central unit.

Results and discussion

In this chapter, the synthesis and mesomorphic properties of a number of homologous series of compounds derived from 2,7-dihydroxynaphthalene have been described. In addition, several compounds derived from resorcinol have also been synthesized for comparison. All

these compounds are stable esters without Schiff's base units. Both E-p-n-alkoxycinnamic acids and E-p-n-alkoxy-α-methylcinnamic acids have been used in the arms of these bent-core compounds. These have resulted in many interesting mesophases including a novel two-dimensional columnar antiferroelectric phase with an oblique lattice. The first observation of a direct transition from the antiferroelectric B_2 phase to a nematic phase is reported. In addition, a direct transition from a nematic phase to a columnar phase with an oblique lattice was also obtained. As discussed in Chapter-**2**, the influence of a fluorine substituent on the phenyl rings in the side arms of these compounds have also been examined. The nematic phase has been obtained exclusively in compounds derived from 2,7-dihydroxynaphthalene.

All these bent-core compounds were prepared using a general synthetic pathway shown in scheme **3.1**. The general molecular structure representing the different homologous series investigated is shown in structure **3.I**.

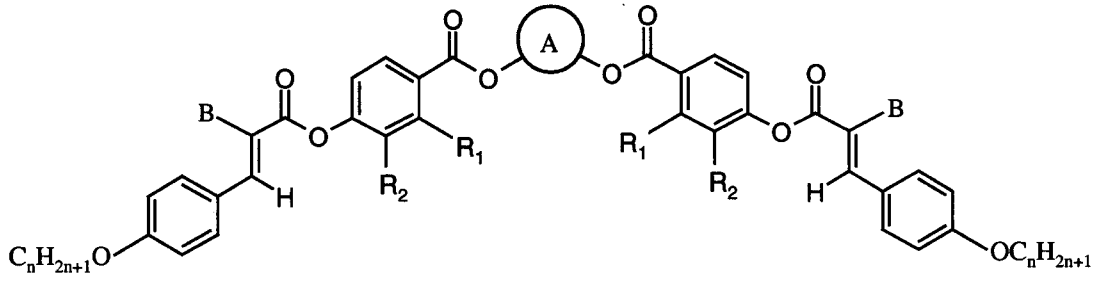

A= 2,7-Naphthylene, B=H; R_1=F, R_2=H	Series - **3.I**
A= 2,7-Naphthylene, B=CH_3; R_1=F, R_2=H	Series - **3.II**
A= 2,7-Naphthylene, B=H; R_1=H, R_2=F	Compound **3.C.1**
A= 2,7-Naphthylene, B=CH_3; R_1=H, R_2=F	Series - **3.III**
A= 2,7-Naphthylene, B=CH_3; R_1=H, R_2=H	Compound **3.E.1**
A= 1,3-Phenylene, B=H; R_1=F, R_2=H	Series - **3.IV**
A= 1,3-Phenylene, B=CH_3; R_1=F, R_2=H	Series - **3.V**

Structure 3.I

The commercially obtained 2,7-dihydroxynaphthalene was purified before use. 4-Benzyloxybenzoic acid, 2-fluoro-4-benzyloxybenzoic acid and 3-fluoro-4-benzyloxybenzoic acids were prepared as described in Chapter-**2**. The E-4-n-alkoxycinnamic acids were prepared following a procedure described by Gray and Jones [96]. The E-4-n-alkoxy-α-methylcinnamic acids were prepared according to the procedure described by Johnson [97]. The transition temperatures obtained for the compounds of these homologous series agree with the reported values [98]. As shown in scheme **3.1**, esterification of 1,3-dihydroxy-benzene or 2,7-dihydroxynaphthalene using two equivalents of 2-fluoro- or 3-fluoro-4-benzyloxybenzoic acid yields the dibenzyloxy ester. The target materials were obtained by hydrogenolysis of benzyloxy esters in the presence of 5% Pd-C as a catalyst in an hydrogen atmosphere followed by the esterification of bis-phenols obtained (**3.1**, **3.2**, **3.3** and **3.5**) with two equivalents of E-4-n-alkoxy-cinnamic or α-methylcinnamic acids.

The phase transition temperatures and the associated enthalpy values for the different homologous series of bent-core compounds synthesized viz. series **3.I**, **3.II**, **3.III**, **3.IV** and **3.V** are summarized in tables **3.1**, **3.3**, **3.5**, **3.6** and **3.7** respectively. A total of 38 compounds have been synthesized, characterized and are described in this chapter. Among these, three are non-mesomorphic, two are trimesomorphic, 23 are dimesomorphic and the rest exhibit monomesomorphism. In general, the liquid crystalline properties exhibited by these compounds have been investigated by the usual techniques of polarized light optical microscopy, differential scanning calorimetry and X-ray diffraction studies. Triangular-wave method was employed to determine the ground state mesophase structure and to measure the spontaneous polarization in antiferroelectric phases.

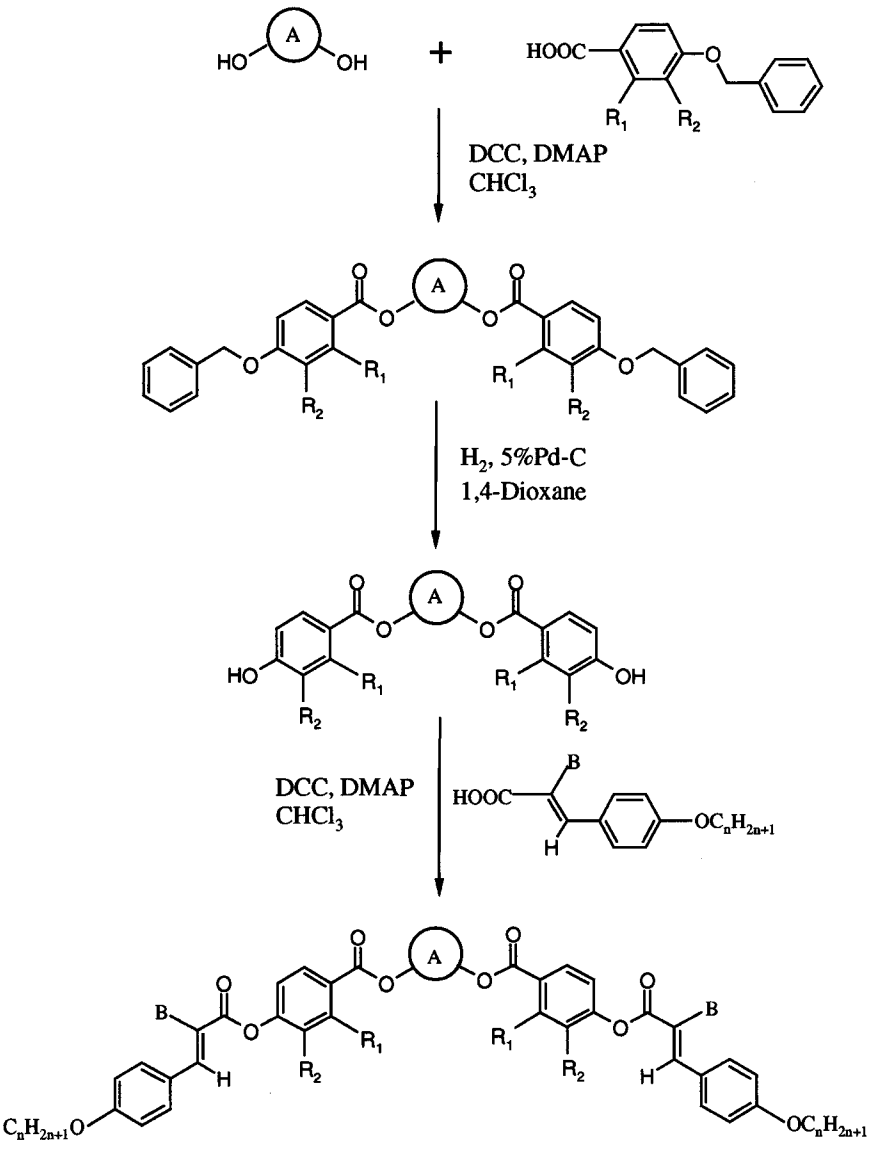

A=1,3-Phenylene or 2,7-Naphthylene; B=H or CH_3; R_1, R_2=H or F

Scheme 3.1. General synthetic pathway used for the preparation of bent-core mesogens derived from 1,3-dihydroxybenzene or 2,7-dihydroxynaphthalene.

Mesomorphic properties of compounds of series 3.I:

The phase transition temperatures and the associated enthalpies obtained for the compounds of series **3.I** are summarized in table **3.1**. It can be seen that five enantiotropic mesophases have been obtained by the variation of n-alkoxy chain length. Among these, four show B-phases and the other exhibits a nematic phase.

The lower homologues namely, compounds **3.A.1** and **3.A.2** show two banana phases in addition to the nematic phase. Compound **3.A.2** shows the following textural features under a polarizing microscope. On cooling the isotropic liquid, nematic phase develops in which ±1 as well as ±1/2 strength defects could be seen, which is an evidence for the uniaxiality of the phase. On further cooling to a temperature of about 187°C, colourful batonnets grow and immediately transform to a fan-shaped texture. This mesophase could never be aligned homeotropically, thus the possibility of SmA phase can be excluded and the mesophase has been identified as a B_6 phase. On lowering the temperature further, this mesophase transforms to a higher ordered mesophase with a minimal textural change. The phase transition is weakly first order (about 0.1 to 0.4 $kJmol^{-1}$). On shearing the coverslip, this mesophase displays a mosaic texture which is the typical feature of a B_1 phase. The textural change accompanying the phase transitions on lowering the temperature from N to B_6 is shown in figure **3.1a** and the textures of B_6 and B_1 phases are shown in figure **3.1 b** and **c** respectively. Perhaps these represent only the second example of compounds showing a direct transition from the nematic to a B_6 phase. The first example of compounds have already been described in Chapter-**2**. On increasing the terminal chain length, the core-core and the chain-chain interactions increase and hence a few BC molecules join together to form clusters. These clusters arrange themselves to form a lattice such that they stabilize the columnar phase and hence only a N to B_1 phase transition is observed for compounds **3.A.3** and **3.A.4**. Interestingly, the direct transitions from N to B_6 and N to B_1 phases could be obtained on ascending the homologous series. From the X-ray diffraction data, as shown in figure **3.2**, the values of (11) plane in the B_1 phase rises while the values of (02) plane increase gradually on ascending the homologous series. The values of these two sets of planes cross over at compound **3.A.3**. Hence, the reflections obtained for the mesophase of this compound can be indexed for a hexagonal lattice. However, this is not a true hexagonal phase and can be obtained from a rectangular lattice when the lattice parameter $\mathbf{b}=\sqrt{3}\,\mathbf{a}$. Thus, for compound **3.A.4,** the first two reflections exchange when compared with the lower homologues.

Table 3.1. Transition temperatures (°C) and enthalpies (kJmol^{-1}) (*in italics*) for compounds of series 3.I.

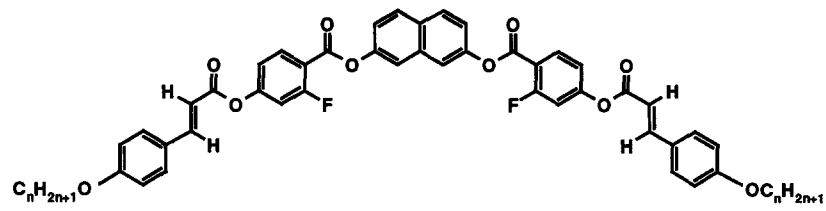

Compound	n	Cr	B_{X4}	B_{X3}	B_1	B_6	N	I
3.A.1	5	. 175.0	-	-	. 178.5	. 203.0	. 225.0	.
		55.6			*0.12*	*10.1*	*0.89*	
3.A.2	6	. 148.5	-	-	. 183.5	. 188.0	. 211.0	.
		42.2			*0.36*	*9.6*	*0.66*	
3.A.3	7	. 135.5	-	-	. 174.0	-	. 196.0	.
		46.1			*13.1*		*0.53*	
3.A.4	8	. 136.0	-	-	. 162.0	-	. 187.5	.
		49.8			*11.4*		*0.55*	
3.A.5	9	. 124.5	-	. 153.5	-	-	. 181.0	.
		40.5		*11.5*			*0.52*	
3.A.6	10	. 122.0	-	. 145.0	-	-	. 176.0	.
		53.6		*11.1*			*0.53*	
3.A.7	11	. 126.5	-	. 147.0	-	-	. 170.5	.
		56.7		*10.9*			*0.46*	
3.A.8	12	. 126.5	-	. 152.0	-	-	. 168.5	.
		43.8		*13.1*			*0.45*	
3.A.9	14	. 125.0	-	. 160.5	-	-	. 163.5	.
		62.4		*14.4*			*0.43*	
3.A.10	16	. 121.0	-	. 168.5	-	-	-	.
		68.4		*17.3*				
3.A.11	18	. 118.5	. 125.0	. 172.5	-	-	-	.
		76.1	*0.45*	*18.7*				

Key: Applicable to all tables: Cr=Crystalline phase; N=Nematic phase; B_1=Two-dimensional rectangular columnar phase; B_2=Lamellar antiferroelectric banana phase; B_6=Intercalated smectic banana phase; B_{X3}=Novel two-dimensional columnar banana phase with an oblique lattice; B_{X4}=More ordered columnar phase with an oblique lattice; B_{X5}=Novel antiferroelectric two-dimensional columnar phase with an oblique lattice. I=Isotropic phase; . Phase exists; - Phase does not exist; Temperature in parentheses indicate monotropic transitions.

(a)

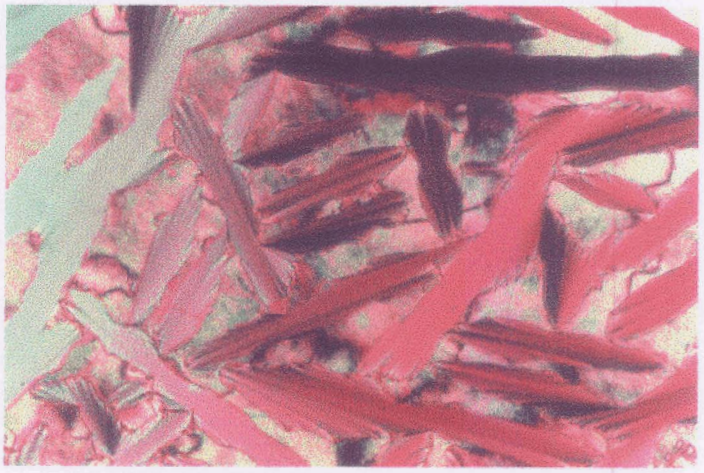

(b)

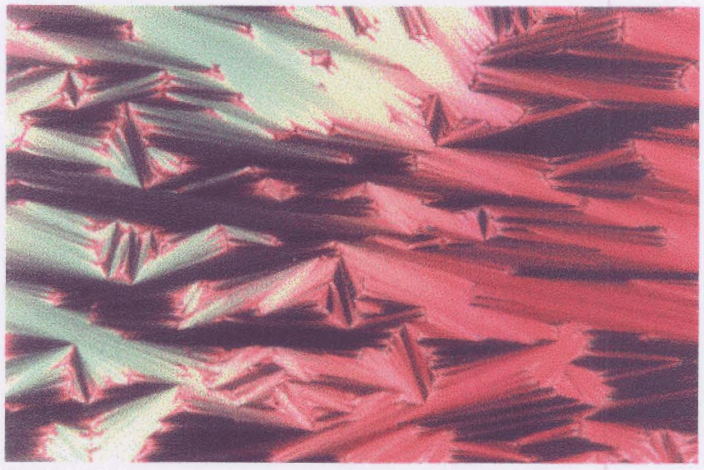

(c)

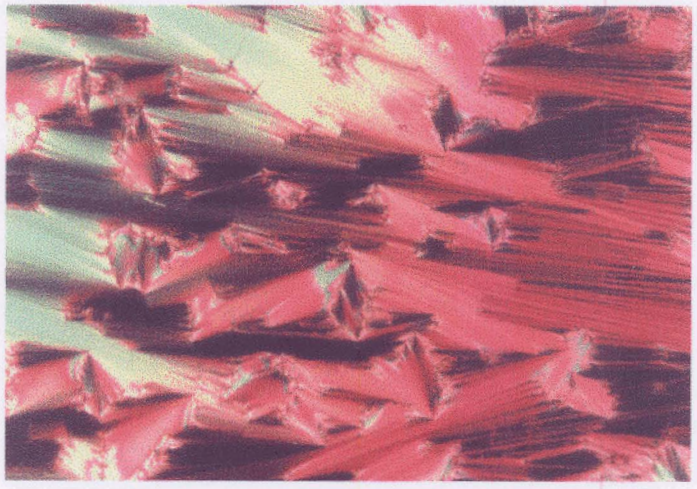

Fig. 3.1. Optical photomicrographs obtained for compound 3.A.2, (a) a B_6 phase developing from the nematic phase, (b) completely formed B_6 phase and (c) B_1 phase obtained, same region as in (b).

Table 3. 2. The d-spacings (Å) obtained for different mesophases and the corresponding Miller indices shown in brackets for the compounds of homologous series 3.I. The XRD measurements have been carried out on mesophases obtained on cooling. (In the B_1 phase, 'b' corresponds to the length of the molecule while in the B_{X3} phase, 'a' corresponds to the length of the molecule).

Comp-ound	d-spacings Å / Miller indices	Lattice parameters/ Å		Phase type	Oblique angle β (deg.)
		a	b		
3.A.1	22.1 (01), 11.1 (02)	-	-	B_6	-
	22.1 (02), 20.8 (11), 12.5 (13), 11.1 (04)	23.6	44.2	B_1	-
3.A.2	23.0 (01), 11.5 (02)	-	-	B_6	-
	23.0 (02), 22.1 (11), 13.0 (13), 11.5 (04)	25.1	46.0	B_1	-
3.A.3	23.5 (02 & 11), 13.4 (13), 11.8 (04)	-	-	B_1	-
3.A.4	24.7 (11), 24.2 (02), 14.1 (20), 12.1 (04)	28.7	48.5	B_1	-
3.A.5	28.0 (10), 24.4 (11), 22.0 (01)	32.6	25.6	B_{X3}	59.2
3.A.6	29.5 (10), 22.9 (11), 18.7 (01)	36.2	23.0	B_{X3}	55
3.A.7	31.3 (10), 22.2 (11), 18.0 (01), 15.9 (20), 12.8 (31), 10.7 (30), 9.2 (42)	38.6	22.2	B_{X3}	54
3.A.8	32.8 (10), 21.6 (11), 17.3 (01), 13.8 (31), 9.4 (42)	41.1	21.7	B_{X3}	53
3.A.9	35.6 (10), 21.4 (11), 17.1 (01), 14.8 (31)	45.2	21.7	B_{X3}	52
3.A.11	39.8 (10), 19.8 (11), 18.3 (01)	43.2	19.8	B_{X3}	67.2
	(or)				
	39.8 (10), 19.8 (01), 18.3 (11)	39.9	19.9	B_{X3}	85.6
3.A.11	40.2 (10), 20.6 (11), 17.5 (01), 15.9 (31)	47.6	20.8	B_{X4}	57.5
	(or)				
	40.2 (10), 20.6 (01), 17.5 (11), 15.9 (21)	40.5	20.8	B_{X4}	96.9

This indicates that the number of molecules that exist in each cluster increases on increasing the chain length. However, the textures obtained for the higher homologues (compounds **3.A.5** to **3.A.11**) are somewhat similar to a columnar B_1 phase but distinguishable features could be clearly seen. On cooling the nematic phase of compound **3.A.9**, flower-like pattern develops as shown in figure **3.3a** and this transforms to an undefined texture on lowering the temperature. A growth of small mosaic-like pattern could also be seen. Compound **3.A.10** exhibits spherulitic growth pattern in addition to the more complex textural pattern as shown

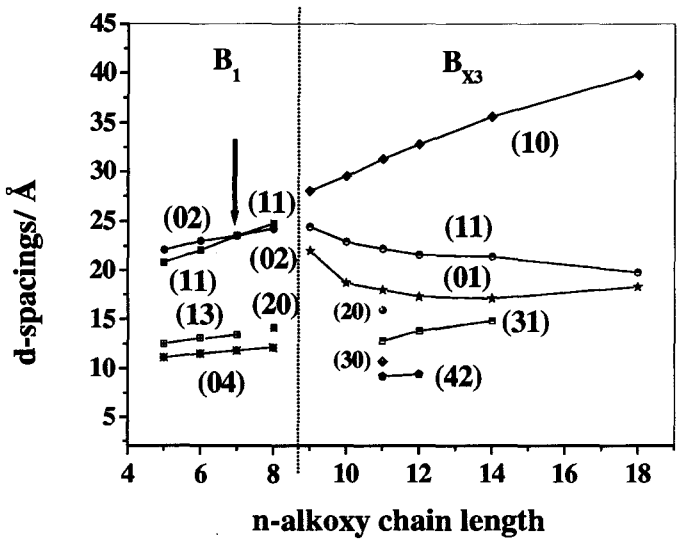

Fig. 3.2. Plot of d-spacings as a function of n-alkoxy chain length obtained for the compounds of series 3.I. The change in the XRD pattern could be clearly seen between B_1 and B_{X3} phases. The arrow shows the homologue at which the (11) and (02) reflection planes cross in the B_1 phase on ascending the series.

in figure **3.3** (**b** & **c**). This mesophase has been designated as B_{X3}. X-Ray diffraction studies have been carried out for most of the compounds exhibiting B_{X3} mesophase and are summarized in table **3.2**. These reflections cannot be indexed to a simple rectangular lattice as in the case of B_1 phase. However, these reflections can be indexed for an oblique lattice as follows. Compound **3.A.7** shows seven reflections in the small angle region. The first three reflections obtained at d_1=31.3 Å, d_2=22.2 Å and d_3=18 Å can be assumed as (10), (11) and (01) respectively for an oblique lattice. The lattice parameters obtained are **a**=38.6 Å and **b**=22.2 Å and the oblique angle β is 54°. Using these parameters, the remaining four reflections at d_4=15.9 Å, d_5=12.8 Å, d_6=10.7 Å and d_7=9.2 Å can be indexed as (20), (31), (30) and (42) respectively (calculated values: 15.7Å (20), 12.9Å (31), 10.4Å (30) and 9.1Å (42) respectively) for an oblique lattice. Similarly, the d-spacings obtained for other compounds exhibiting the B_{X3} phase can be indexed for an oblique lattice as shown in table **3.2**. The X-ray angular intensity profile obtained in the B_{X3} phase of compound **3.A.8** is shown in figure **3.4**. The wide-angle diffuse peak obtained at about 4.8 Å suggests the absence of in-plane order. The B_{X3} to isotropic transition enthalpy value is not very high and varies from 11 to 19 $kJmol^{-1}$. No electro-optical switching could be observed in B_{X3} mesophase even at triangular-wave electric field of about $\pm 30 V \mu m^{-1}$.

(a)

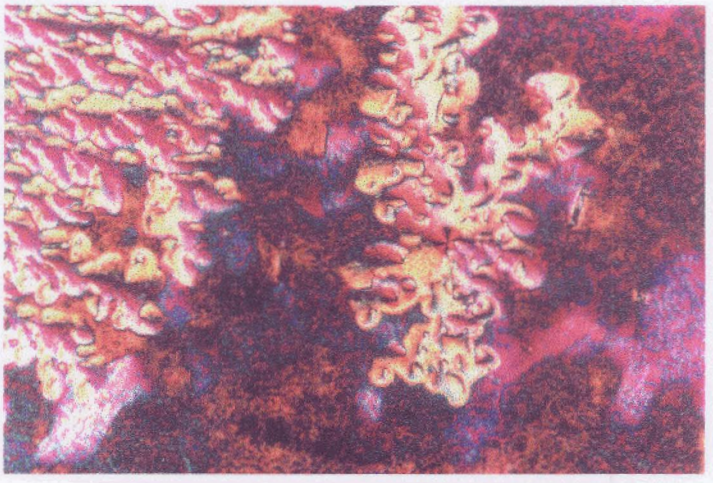

(b)

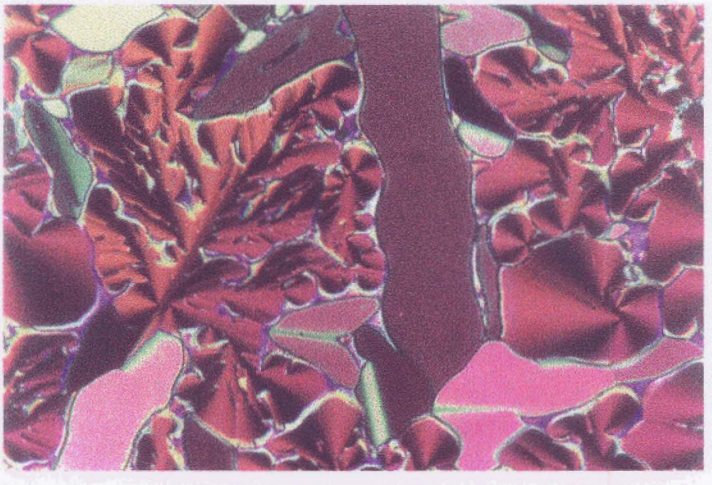

(c)

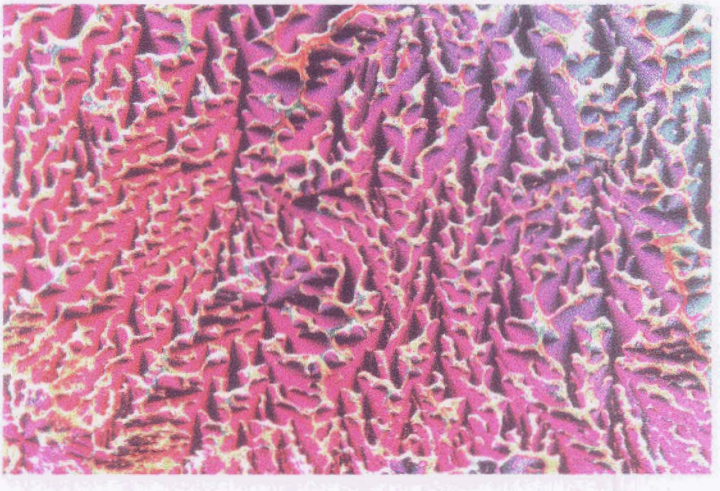

Fig. 33. Optical photomicrographs of (a) flower-like pattern of the B_{X3} phase growing from a nematic phase of compound 3.A.9, (b) tiny mosaics and spherulitic growth patterns obtained in the B_{X3} mesophase exhibited by compound 3.A.10 and (c) more complex textural pattern obtained for compound 3.A.10.

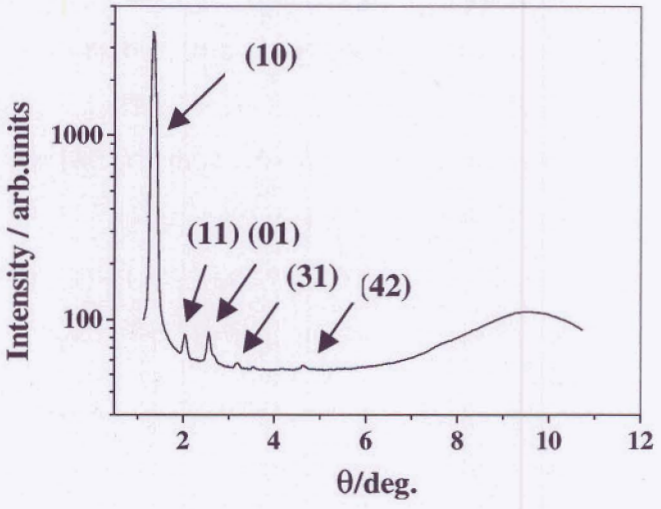

Fig. 3.4. X-Ray angular intensity profile obtained in the B_{X3} mesophase exhibited by compound 3.A.8.

(a)

(b)

Fig. 3.5. Photomicrographs obtained for compound 3.A.11 (a) B_{X3} mesophase and (b) B_{X4} mesophase (same region as in (a)).

Compound **3.A.11** shows an additional mesophase which appears at a lower temperature w.r.t the B_{X3} phase and has been designated as B_{X4}. The phase transition takes place to the B_{X4} phase with additional sharp lines over the fan-shaped pattern which is present in the B_{X3} phase. The phase transition enthalpy is about 0.4 $kJmol^{-1}$. The optical textural changes observed in B_{X3} and B_{X4} phases are shown in figure **3.5.** The X-ray data obtained in B_{X4} mesophase of compound **3.A.11** can be indexed for an oblique lattice as shown in table **3.2.** However, it is very difficult to differentiate the B_{X4} phase from B_{X3} phase based on X-ray diffraction studies. In addition, no polarization current peak /s were observed up to about ± 40 $V\mu m^{-1}$ in both the B_{X3} and B_{X4} phases.

Figure **3.6** shows a plot of transition temperatures as a function of n-alkoxy chain length for the compounds of series **3.I.** The clearing temperature curves obtained for N and B_6 phases fall steeply while the curve obtained for the B_1 phase rises initially and then falls on ascending the homologous series. However, the clearing temperature curve obtained for B_{X3} phase falls initially and then rises gradually on ascending the homologous series and all the points fall on a smooth curve. Interestingly, the nematic phase exists even for the higher homologues, up to the n-tetradecyloxy derivative which is rather unusual for compounds exhibiting banana phases. As we shall see later, even by shifting the position of fluorine in the middle phenyl ring from *ortho* to *meta* position, similar phase behaviour could be observed (compound **3.C.1)** with minimal change in the transition temperatures.

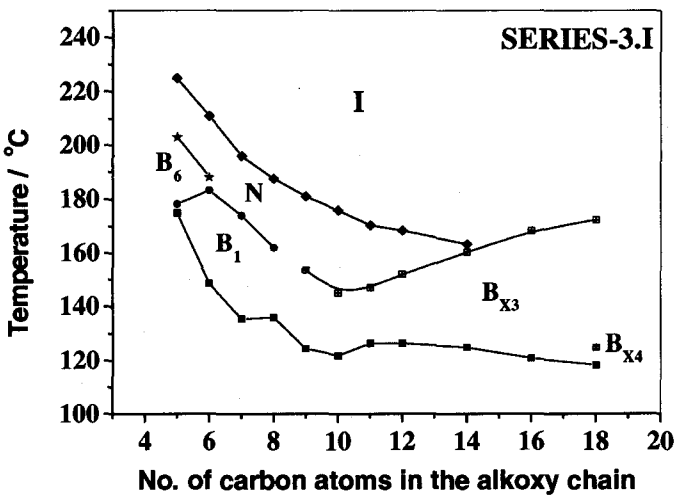

Fig. 3.6. Plot of transition temperatures as a function of n-alkoxy chain length obtained for the compounds of series 3.I.

It is interesting to note that the lower homologues show a B_1 phase with a rectangular lattice while the higher homologues show a columnar phase with an oblique lattice. Thus, the direct

transitions from N to B_1 (rectangular lattice) and N to B_{X3} (oblique lattice) phases have been obtained on ascending the homologous series.

Mesomorphic properties of compounds of series 3.II and 3.III:

An examination of compound **3.B.2** of series **3.II** under a polarizing microscope reveals the following features. On cooling the isotropic liquid, a uniaxial nematic phase appears as indicated by the observation of 2- & 4- brush defects. On cooling the nematic phase, textural pattern of the B_1 phase appears which forms a mosaic texture as shown in figure **3.7**. X-Ray diffraction pattern of an oriented sample of this compound in the B_1 phase shows 6 spots in the small angle region and this is similar to the XRD pattern of a hexagonal columnar phase obtained for disk-like molecules. In addition, two more reflections are obtained in the small angle region and all these are recorded in table **3.4.** These small angle reflections are in the ratio of 1: $1/\sqrt{3}$:1/2 which can be indexed as (01), (11) and (02) respectively for a hexagonal columnar phase. The X-ray angular intensity profile obtained in this mesophase is shown in figure **3.8a**. The wide-angle diffuse peak at about 4.7 Å suggests a liquid-like in-plane order. However, the preferred orientation direction of alkyl chains (as shown in figure **3.8b**) excludes the possibility of a hexagonal columnar phase. This indicates that the (02) and (11) plane reflections due to a rectangular lattice merge for compounds **3.B.1** and **3.B.2**. Thus, the reflections obtained for compounds **3.B.1** and **3.B.2** can be indexed for a rectangular columnar B_1 phase. The orientation direction of the aliphatic chains obtained in the wide-angle region is perpendicular to the layer reflections in the small angle region. This probably indicates the orthogonal arrangement of the molecules in the B_1 phase.

On ascending the homologous series, compounds **3.B.3** to **3.B.6** show textural patterns similar to those of a B_1 phase and the X-ray data obtained can be indexed for a rectangular unit cell as shown in table **3.4.** The X-ray angular intensity profile obtained in the B_1 phase exhibited by compound **3.B.5** is shown in figure **3.9**. On ascending the homologous series the B_1 phase obtained for homologues with shorter chain lengths gets eliminated. For example, compound **3.B.7** exhibits only a nematic phase.

The higher homologues namely, **3.B.8** to **3.B.11** show a banana phase along with the nematic phase. For example, on slow cooling of the isotropic liquid of compound **3.B.10** shows a nematic phase, with an unusual texture (striped pattern) and a photomicrograph of this is

Table 3.3. Transition temperatures (°C) and enthalpies ($kJmol^{-1}$) (*in italics*) for compounds of series 3.II.

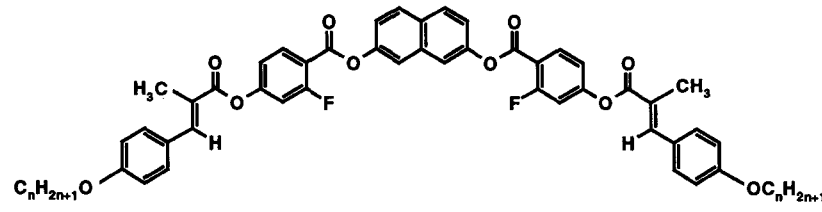

Compound	n	Cr	B_2	B_1	N	I
3.B.1	4	. 143.5	-	(. 140.5)	. 184.0	.
		44.8		*10.6*	*0.75*	
3.B.2	5	. 133.0	-	. 138.0	. 164.0	.
		31.3		*10.4*	*0.57*	
3.B.3	6	. 128.5	-	. 134.0	. 159.0	.
		38.3		*9.7*	*0.53*	
3.B.4	7	. 133.5	-	(. 126.5)	. 148.5	.
		72.1		*11.8*	*0.55*	
3.B.5	8	. 121.5	-	(. 118.5)	. 145.0	.
		62.2		*11.0*	*0.45*	
3.B.6	9	. 118.0	-	(. 109.5)	. 137.0	.
		60.1		*9.9*	*0.43*	
3.B.7	10	. 116.5	-	-	. 134.0	.
		63.4			*0.46*	
3.B.8	11	. 111.5[b]	(. 110.5)[†]	-	. 130.5	.
		101.2	*12.3*		*0.49*	
3.B.9	12	. 119.5	(. 116.0)	-	. 127.0	.
		75.6	*13.2*		*0.49*	
3.B.10	13	. 117.5	. 120.0	-	. 125.0	.
		59.3	*13.9*		*0.43*	
3.B.11	14	. 107.0	. 123.0	-	. 124.0	.
		58.6	*14.1*		*0.34*	
3.B.12	16	. 108.0	. 128.0	-	-	.
		52.4	*16.8*			
3.B.13	18	. 109.0[b]	. 132.0	-	-	.
		115.3	*15.9*			

b : compound has crystal-crystal transition; enthalpy denoted is the sum of all previous transitions.

† : temperature obtained on cooling.

(a)

(b)

Fig. *3.7.* Optical photomicrographs obtained for compound 3.B.2 (a) a B_1 mesophase growing from the nematic phase and (b) completely formed uniform mosaic texture of the B_1 phase.

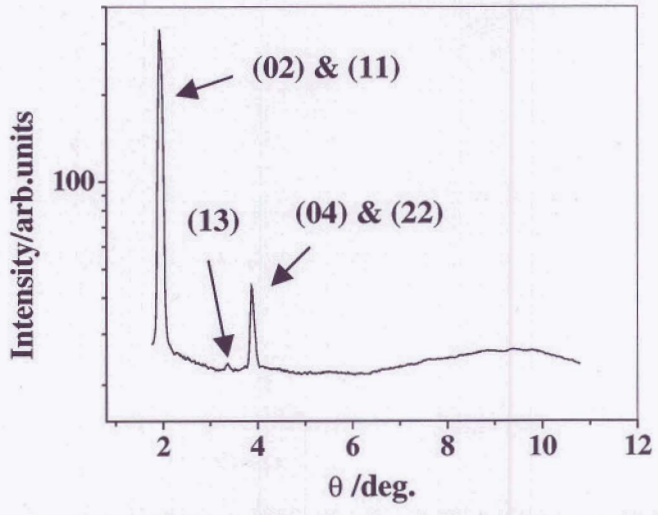

Fig. 3.8a. The X-ray angular intensity profile obtained for compound 3.B.2 in the B_1 mesophase.

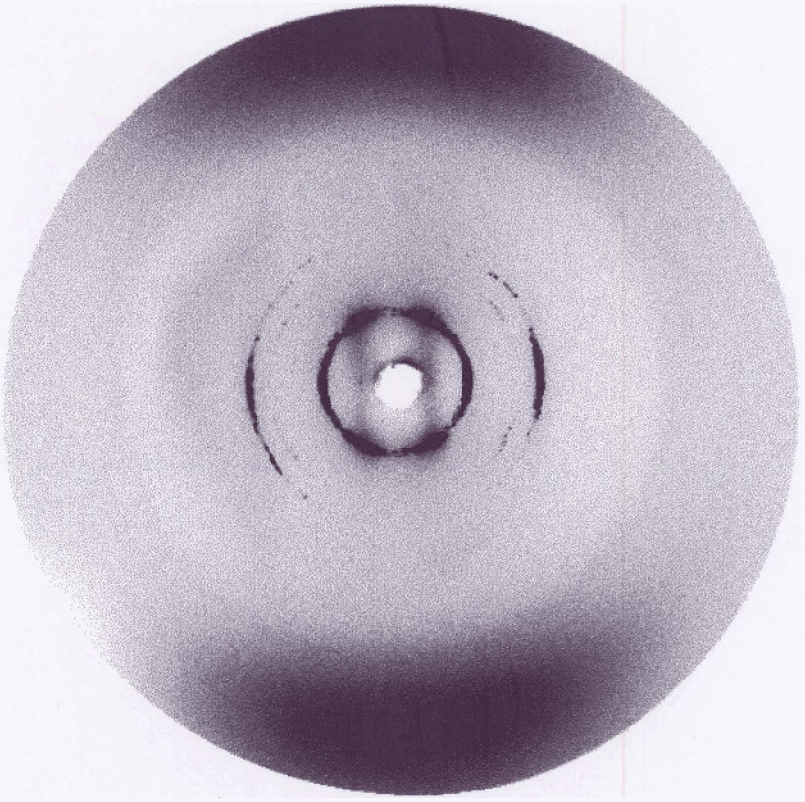

Fig. 3.8b. The oriented X-ray pattern obtained in the B_1 mesophase of compound 3.B.2 indicating the orthogonal arrangement of the molecules in a rectangular lattice.

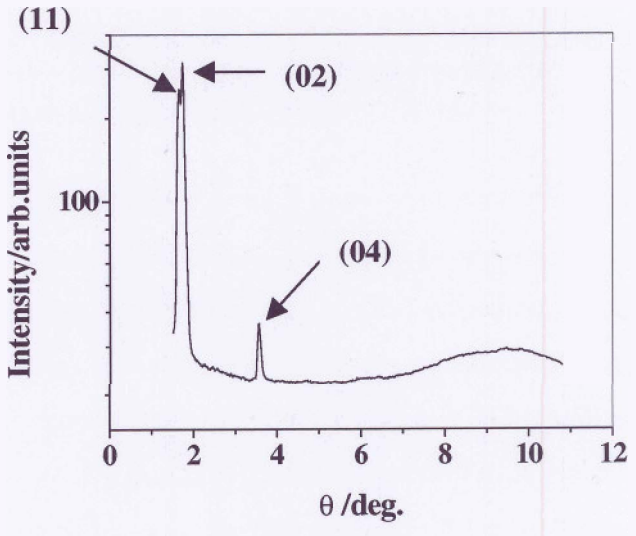

Fig. 3.9. The X-ray angular intensity profile obtained in the B_1 phase of compound 3.B.5 showing a splitting in the first order reflection.

(a)

(b)

Fig. 3.10. Photomicrographs obtained for compound 3.B.10 , (a) the unusual textural pattern obtained in the nematic phase and (b) small broken fan-like texture of B_2 phase developing from a homogeneously aligned nematic phase.

shown in figure **3.10a.** *On* further slow cooling, fingerprint texture emanates from the nematic phase and the whole field of view is filled completely with this texture. This textural feature is indicative of a lamellar B_2 phase. The clearing transition enthalpy value obtained is in the range of 12-16 $kJmol^{-1}$ which is expected for a B_2 phase. However, the nematic phase obtained could never be aligned homeotropically even in cells treated for such an alignment. In contrast, this aligns very well in a homogeneous geometry. A photomicrograph of the B_2 phase growing from a homogeneously aligned nematic phase is shown in figure **3.10b.** On ascending the homologous series, the nematic phase gets eliminated and only the B_2 phase is stabilized as observed for compounds **3.B.12** and **3.B.13**. The X-ray diffraction pattern obtained in the mesophases of unoriented samples of compounds **3.B.10, 3.B.11** and **3.B.13** show lamellar reflections in the small angle region and a diffuse peak in the wide-angle region

at about 4.6 Å, indicating the absence of in-plane order. The calculated tilt angle is about 50°. A plot of the d-spacings as a function of the terminal chain length obtained for this homologous series is shown in figure **3.11.**

Finally, the characteristic feature of the B_2 phase, namely, the switching current response was obtained for compound **3.B.11.** The sample was filled in the isotropic phase and cooled slowly to obtain a very good alignment of the nematic phase. On cooling the nematic phase further under a triangular-wave voltage and at a low frequency, well-aligned domains of the B_2 phase over the entire field of view could be seen. Observation of two sharp current peaks for half period of the triangular voltage (±21 $V\mu m^{-1}$, 29 Hz) confirms the antiferroelectric ground state of the B_2 phase. A typical switching current response obtained for this compound is shown in figure **3.12.** The apparent saturated polarization value (P_s) obtained by measuring the area under the current peaks is about 560 nC cm^{-2}.

A plot of the transition temperatures as a function of n-alkoxy chain length obtained for the compounds of homologous series **3.II** is shown in figure **3.13.** The N-I transition temperatures gradually decrease on increasing the chain length. The B_1-I transition temperatures curve falls steeply while the clearing temperature points for the B_2 phase rises initially and lie on a smooth curve on ascending the homologous series.

Table 3.4. The d-spacings (Å) obtained for different mesophases and the corresponding Miller indices shown in brackets for the compounds of homologous series 3.II. The XRD measurements have been carried out on the mesophases obtained on cooling.

Compound	d-spacings Å / Miller indices	Lattice parameters/ Å		Phase type	T/ °C
		a	**b**		
3.B.1	21.3(02)&(11), 12.3(13), 10.7(04)&(22)	24.6	42.6	B_1?	137
3.B.2	22.1(02)&(11), 12.9(13), 11.0(04)&(22)	25.5	44.2	B_1?	135
3.B.3	24.0 (11), 22.9 (02), 13.4 (13), 11.5 (04)	28.2	45.8	B_1	130
3.B.4	25.3 (11), 23.5 (02), 14.0 (13), 11.8 (04)	30.0	47.0	B_1	124
3.B.5	26.3 (11), 24.2 (02), 12.3 (04)	31.2	48.4	B_1	116
3.B.10	39.2 (01), 19.7 (02)	-	-	B_2	117
3.B.11	40.6 (01), 20.3 (02)	-	-	B_2	115
3.B.13	44.3 (01), 22.5 (02), 14.9 (03)	-	-	B_2	120

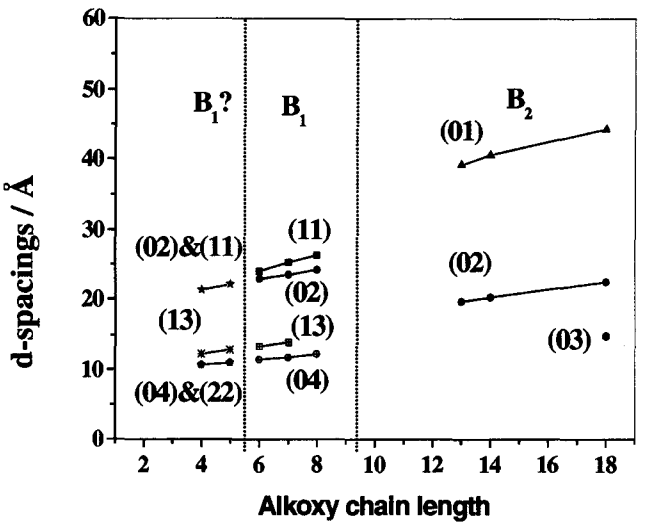

Fig. 3.11. Plot of d-spacings as a function of n-alkoxy chain length obtained in the mesophases exhibited by compounds of series 3.II.

By changing the position of the fluorine in the middle phenyl ring from *ortho* to *meta* position, the mesomorphic behaviour is retained with marginal changes in the transition temperatures (series **3.III**). As can be seen in table **3.5**, compound **3.D.1** shows the columnar B_1 phase in addition to the nematic phase. The next two higher homologues namely, **3.D.2** and **3.D.3** show a lamellar B_2 phase and a nematic phase. The growth of the nematic phase and its texture indicate the uniaxial character of the phase. On cooling the nematic phase of compounds **3.D.1** and **3.D.3** a transition takes place to a B_1 and a B_2 phases respectively. However, compound **3.D.4** shows only the antiferroelectric B_2 phase. The optical photomicrographs obtained for I-N, N-B_1 and N-B_2 phases are shown in figure **14 (a, b and c)** while a direct transition from the isotropic phase to a B_2 phase and the appearance of schlieren texture obtained for compound **3.D.4** is shown in figure **3.15**. The XRD studies confirmed the existence of a rectangular lattice in the B_1 phase and lamellar ordering in the B_2 phase. As can be seen in this series of compounds, independent of the position of fluorine in the middle phenyl ring, the nematic phase gets stabilized even for the compounds with longer chain lengths.

In order to confirm the antiferroelectric ground state structure in the B_2 phase, triangular-wave method was employed. The X-ray intensity profile and the current response trace obtained for a B_2 phase exhibited by compound **3.D.3** are shown in figures **3.16a** and **3.16b** respectively. Figure **3.17** shows a pictorial representation of the orientation of dipoles (molecules) for each

half cycle of triangular-wave in the B_2 mesophase, which are responsible for the occurrence of two polarization current peaks.

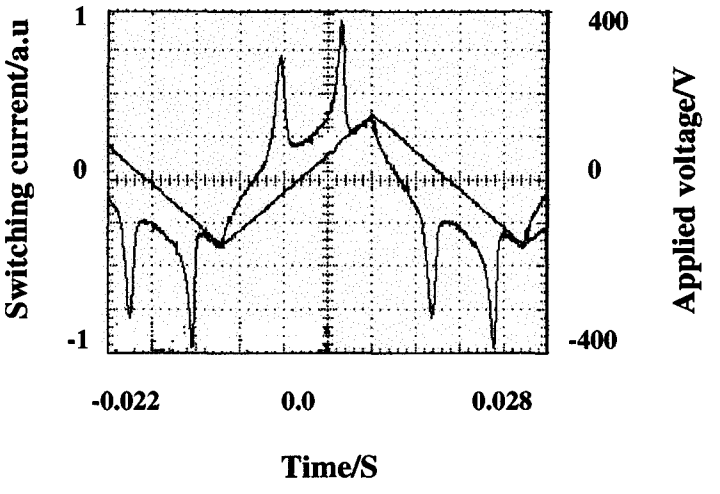

Fig. 3.12. Switching current response obtained in the B_2 mesophase of compound 3.B.11 by applying a triangular voltage (±125V, 29 Hz) at 118°C. Sample thickness 6 *μm*; spontaneous polarization ≈ 560 nC cm^{-2}.

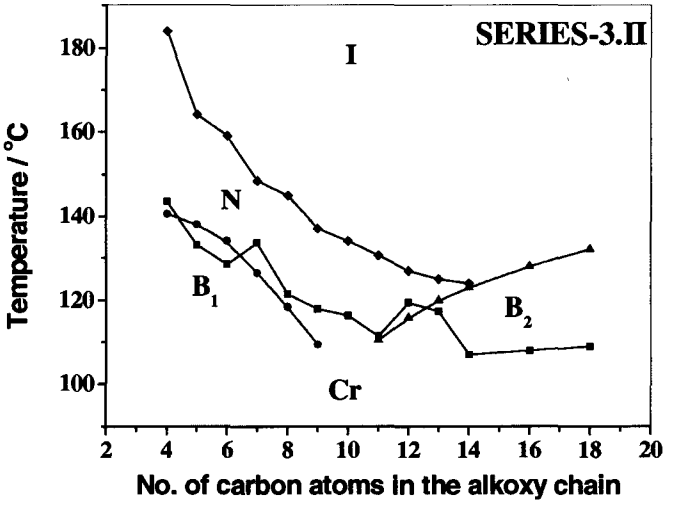

Fig. 3.13. Plot of transition temperatures as a function of n-alkoxy chain length obtained for the compounds of series 3.II.

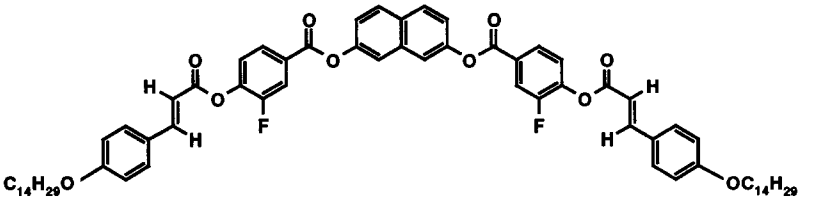

Compound **3.C.1** Cr 142.0 B_{X3} 154.0 N 161.0 I
99.7 *12.7* *0.5*

Table 3.5. Transition temperatures (°C) and enthalpies (kJmol^{-1}) (*in italics*) for compounds of series 3.III.

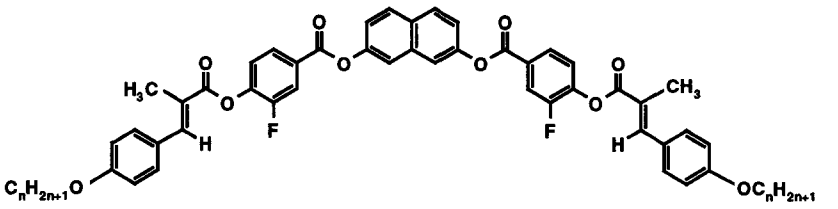

Compound	n	Cr	B_2	B_1	N	I
3.D.1	12	. 111.0	-	. 112.0	. 124.0	.
		44.1		*10.2*	*0.46*	
3.D.2	13	. 112.0	. 114.0	-	. 122.5	.
		90.4	*10.5*		*0.46*	
3.D.3	14	. 102.0	. 117.0	-	. 121.8	.
		55.6	*10.9*		*0.51*	
3.D.4	16	. 107.0	. 122.5	-	-	.
		91.9	*11.7*			

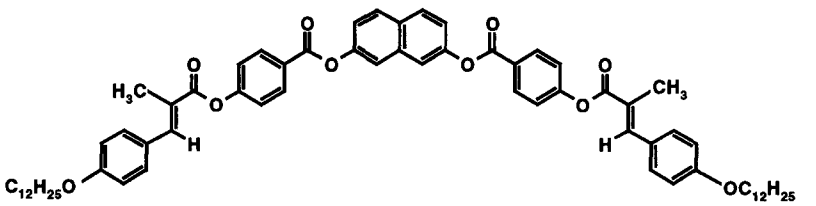

Compound **3.E.1** Cr 143.0 I
95.3

Mesomorphic properties of compounds of series 3.IV and series 3.V:

As observed for the lower homologues of series **3.I**, compound **3.F.1** shows B_6 and B_1 phases which were confirmed by XRD studies as described below. In the small angle region, two sharp reflections were obtained at d_1=21.1 Å, d_2= 10.6 Å and they can be assigned as (01), (02) respectively for a B_6 phase by assuming a tilt of the molecules. On lowering the temperature, a phase transition takes place and four sharp reflections were obtained in the small angle region at d_1=21.1 Å, d_2=18.5 Å, d_3=12.8 Å and d_4=10.6 Å. They can be indexed as (11), (02), (20) and (22) respectively for a rectangular lattice with the lattice parameters, **a**=25.7 Å and **b**=37 Å and the mesophase has been identified as a B_1 phase. It is interesting to note that the d-spacing corresponding to half molecular length (01) obtained in the B_6 phase (21.1Å) decreases in the B_1 phase (18.5Å).

(a)

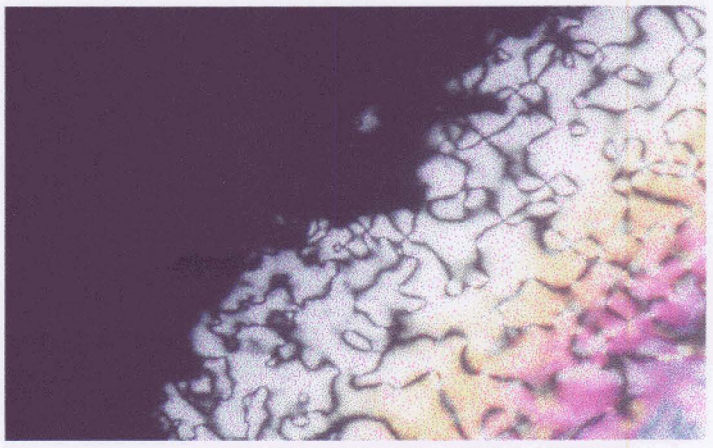

(b)

(c)

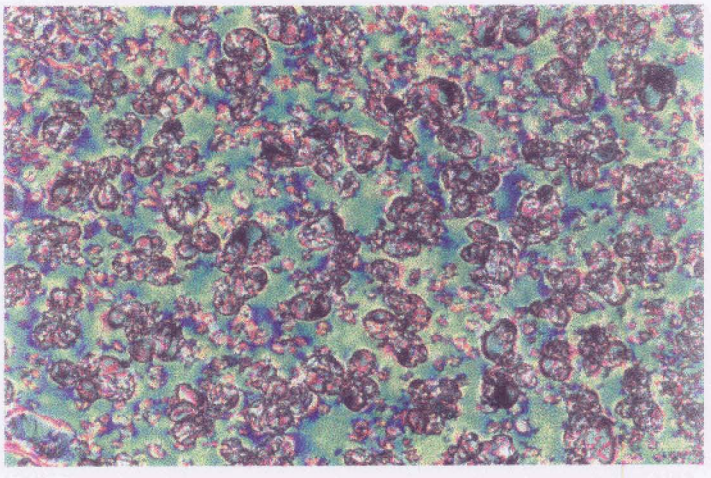

Fig. 3.14. (a) A uniaxial nematic phase developing from the isotropic liquid, (b) transition from the nematic phase to a B_1 phase obtained for compound 3.D.1 and (c) transition from the nematic phase to a B_2 phase obtained for compound 3.D.3.

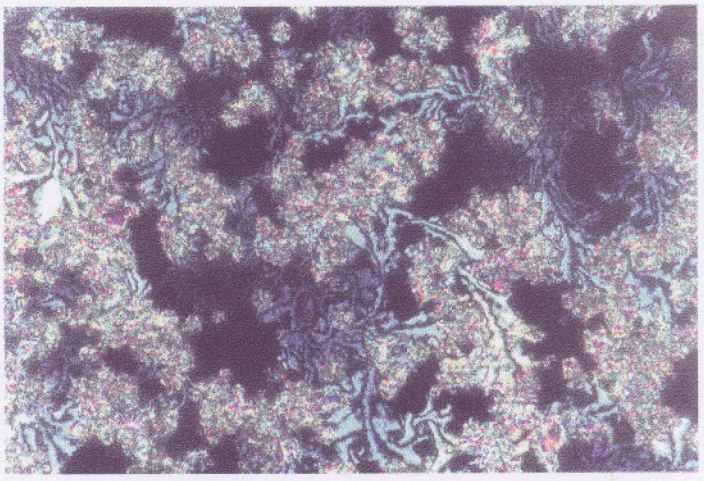

Fig. 3.15. A typical photomicrograph of a schlieren texture of the B_2 phase obtained on cooling the isotropic liquid of compound 3.D.4.

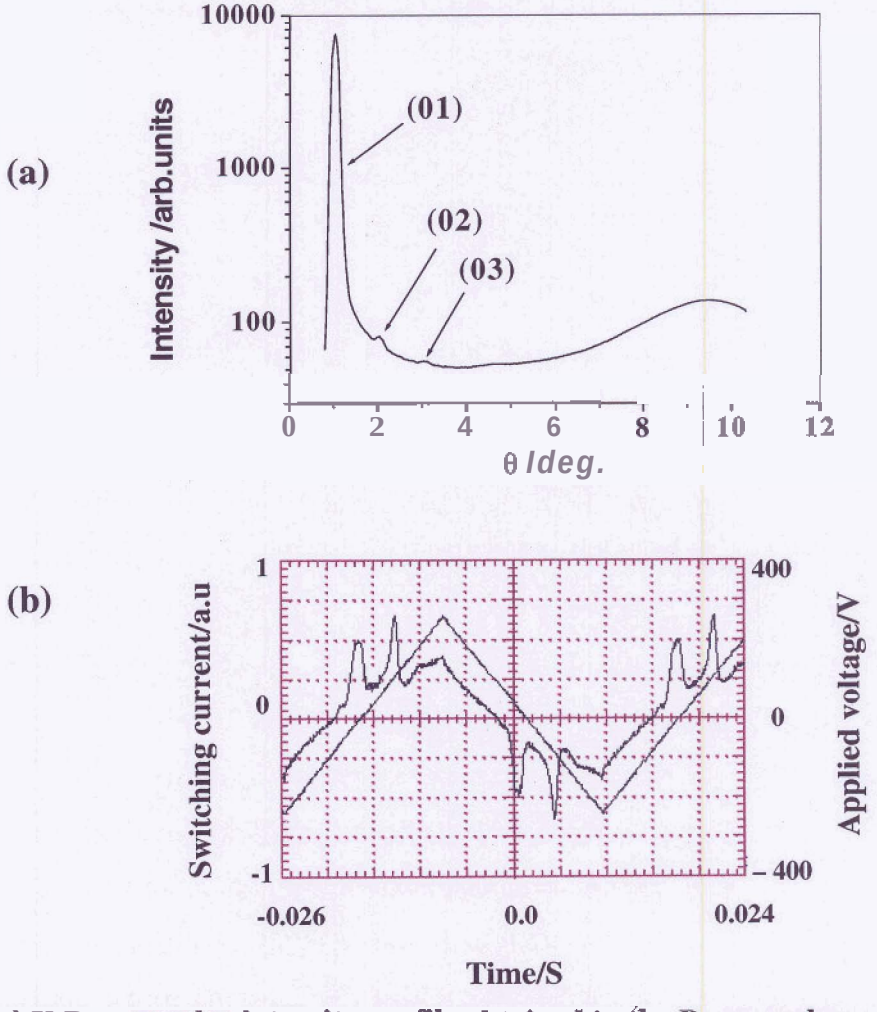

Fig. 3.16. (a) X-Ray angular intensity profile obtained in the B_2 mesophase of compound 3.D.3 and (b) the switching current response obtained in the same compound by applying a triangular voltage (±250V, 30 Hz) at 110%. Sample thickness 9.6 μm; spontaneous polarization ≈ 590 nC cm^{-2}.

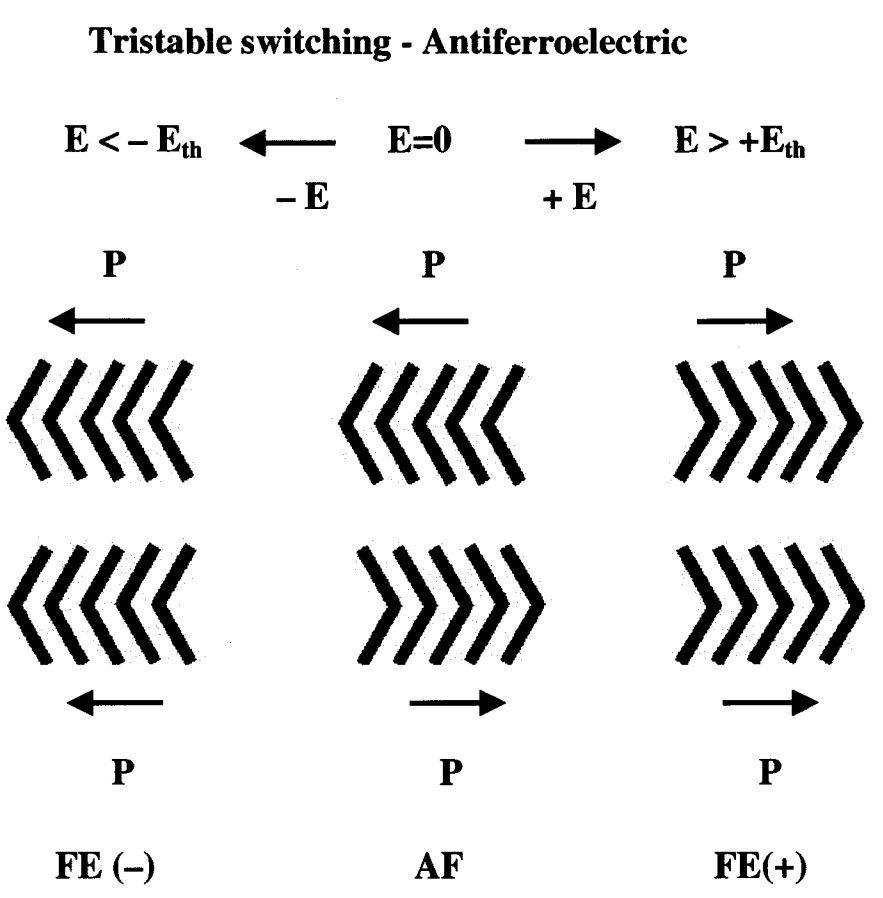

Fig. 3.17. A schematic representation of the arrangement of dipoles under a triangular-wave electric field, which are responsible for the origin of two polarization current peaks indicating the antiferroelectric ground state. E_{th}: threshold voltage, – E_{th}: threshold voltage of opposite polarity.

However, the textural features observed for the higher homologues (**3.F.2** to **3.F.6**) are completely different from the B_6 and B_1 phases and are similar to the textures described for the B_{X3} mesophase phase of the higher homologues of series **3.I**. On slow cooling a thin film of the isotropic liquid of compound **3.F.5,** an unusual complex texture is obtained and a photomicrograph of this is shown in figure **3.18**. Sometimes, this mesophase shows spherulites in addition to small plate-like mosaics. The enthalpy value obtained for this mesophase-isotropic transition varies and is about 10 to 17 $kJmol^{-1}$. This mesophase has been designated as B_{X5}. A plot of the transition temperatures as a function of n-alkoxy chain length obtained for the compounds (**3.F.2** to **3.F.6**) of series **3.IV** is shown in figure **3.19**. The clearing transition temperature (B_{X5}-I) curve gradually rises and then tends to saturate on ascending the homologous series.

Table 3.6. Transition temperatures (°C) and enthalpies (kJmol^{-1}) (*in italics*) for compounds of series 3.IV.

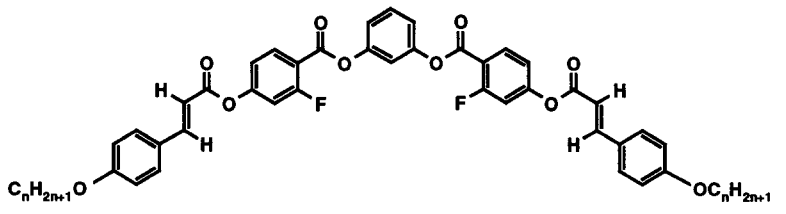

Compound	n	Cr	B_{X5}	B_1	B_6	I
3.F.1	6	. 137.5	-	. 141.0	. 143.0[c]	.
		58.5			*12.1*	
3.F.2	10	. 111.0	(. 98.5)	-	-	.
		49.9	*10.5*			
3.F.3	12	. 110.5	(. 102.0)	-	-	.
		52.2	*11.1*			
3.F.4	14	. 114.5	(. 111.0)	-	-	.
		72.3	*15.9*			
3.F.5	16	. 113.5	. 119.0	-	-	.
		62.5	*17.8*			
3.F.6	18	. 108.0	. 122.0	-	-	.
		127.2	*17.4*			

c: enthalpy denoted is the sum of B_6 to I and B_6 to B_1 phase transitions.

The mesophase of compound **3.F.5** shows the following XRD pattern which cannot be indexed for a rectangular lattice as in the case of B_1 phase. The incommensurate small angle sharp reflections obtained at d_1= 36.8 Å, d_2=19.6 Å, d_3=16.4 Å and d_4=12.8 Å can be indexed as (10), (01), (11) and (21) respectively for an oblique lattice, with the lattice parameters, **a**=37.1 Å and **b**=19.7Å. The oblique angle **β** obtained is 96.9° which is close to a rectangular lattice. Similarly, compound **3.F.6** shows four sharp reflections in the small angle region at d_1=38.4 Å, d_2=19.3 Å, d_3=17.5Å and d_4=14 Å can be indexed as (10), (11), (01) and (21) respectively for an oblique lattice (lattice parameters, **a**=38.4Å and **b**=19.3Å; **β**=88°). A wide-angle diffuse peak at about 4.8 Å obtained in both the compounds suggest the absence of in-plane order.

In addition, the mesophase exhibited by compounds **3.F.2** to **3.F.6** shows an interesting electro-optical switching behaviour. For example, compound **3.F.5** shows two polarization current peaks for each half cycle by applying a triangular-wave electric field of about ±23

$V\mu m^{-1}$ and at a frequency of 30 Hz (threshold voltage ±20 $V\mu m^{-1}$) at 114°C, indicating the antiferroelectric ground state for the mesophase. The calculated spontaneous polarization value is about 350 nC cm^{-2}. The current response trace obtained in this B_{X5} mesophase is shown in figure 3.20. The texture also changes by the application of an electric field. On turning off the applied field, the texture relaxes in which a striated pattern is observed as shown in figure 3.21.

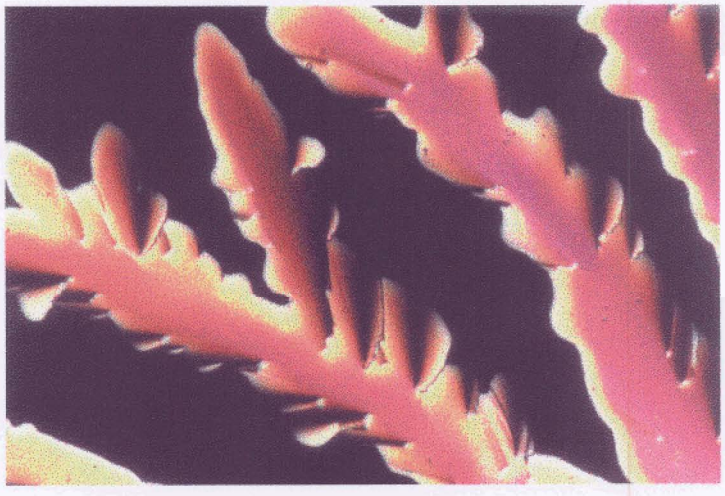

Fig. 3.18. An unusual texture of the B_{X5} mesophase obtained on cooling the isotropic liquid of compound 3.F.5.

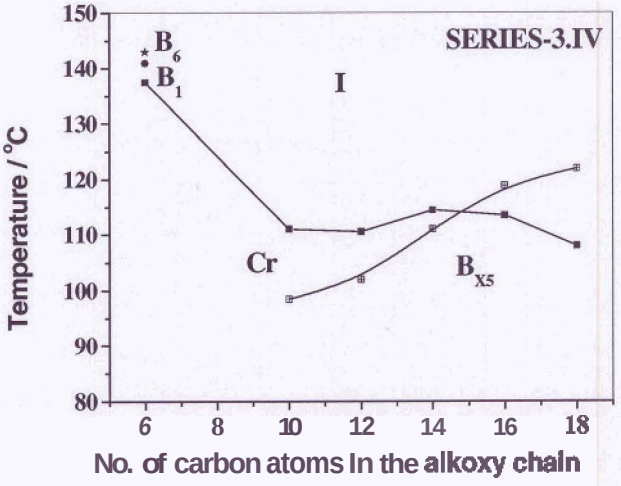

Fig. 3.19. A plot of transition temperatures as a function of terminal chain length obtained for the compounds of series 3.IV.

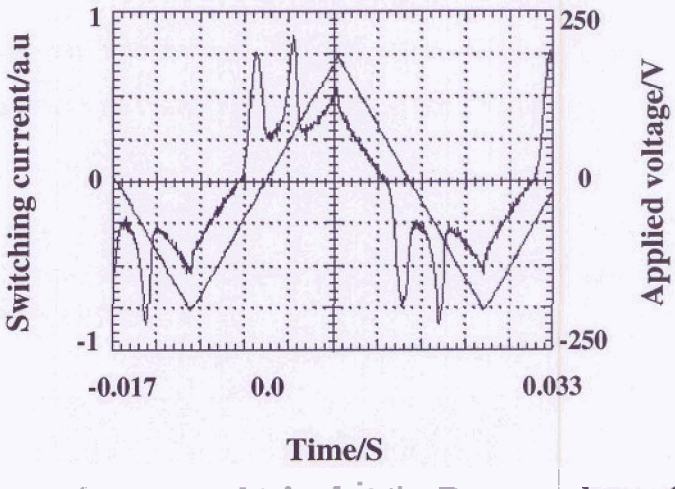

Fig. 3.20. Switching current response obtained in the B_{X5} mesophase of compound 3.F.5 by applying a triangular voltage (±187V, 30 Hz) at 114°C. Sample thickness 8 *μm*; spontaneous polarization ≈ *350* nC cm^{-2}.

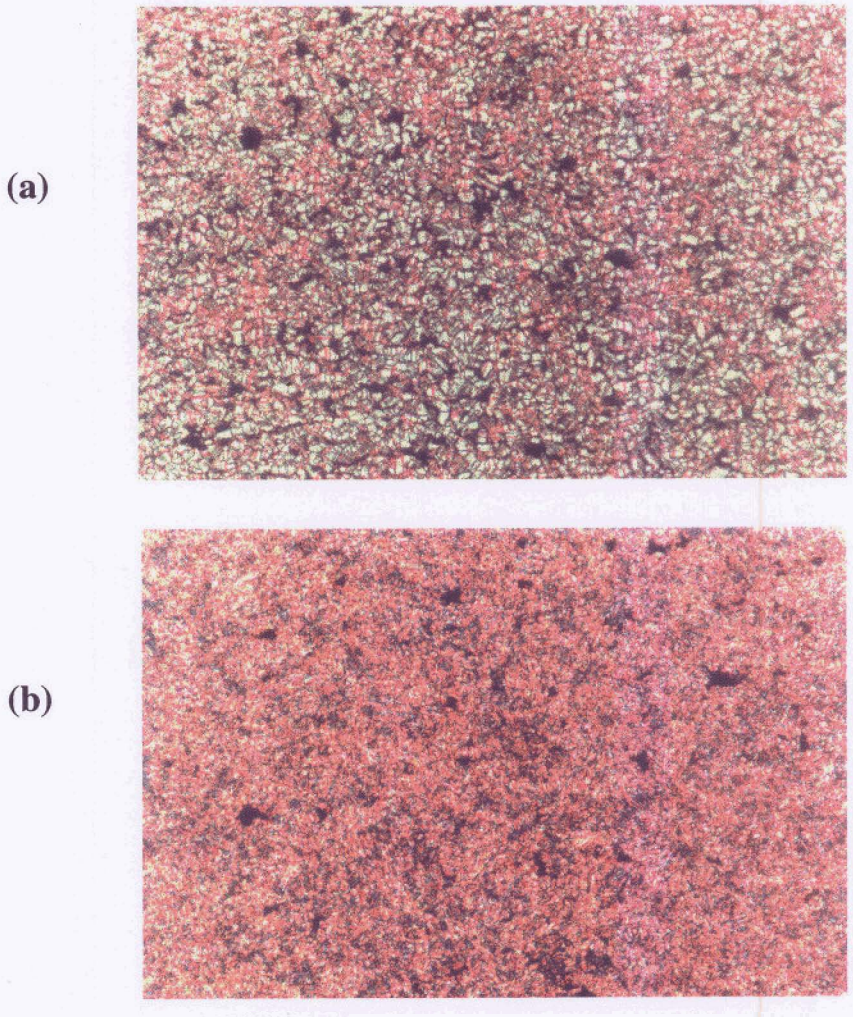

Fig. 3.21. Photomicrographs obtained (a) by the application of triangular-wave electric field in the B_{X5} phase of compound 33.5 (above the threshold voltage) and (b) the same region obtained in absence of the electric field.

However, compounds **3.G.1** and **3.G.2** which contain α-methylcinnamoyloxy groups in the side wings do not show any mesophase. The presence of methyl group in the cinnamoyl moiety of these five-ring esters completely destroys the mesophase probably due to steric reasons.

Table 3.7. Transition temperatures (°C) and enthalpies ($kJmol^{-1}$) (*in italics*) for compounds of series 3.V.

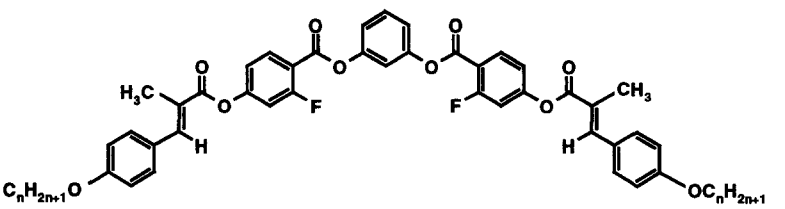

Compound	n	Cr		I
3.G.1	8	.	89.0 *54.4*	.
3.G.2	16	.	96.5 *118.3*	.

Comparison between the mesophases of compounds of series 3.I, 3.II and 3.III:

Compounds of series **3.I**, exhibit 4 different B-phases namely, B_6, B_1, B_{X3} and B_{X4} in addition to a nematic phase. Among these, B_{X3} and B_{X4} phases show an oblique lattice and both of these phases do not switch under a triangular-wave electric field.

In series **3.II**, by introducing a α-methylcinnamoyloxy moiety, the columnar oblique lattice is completely eliminated but a switchable lamellar B_2 phase is induced for the higher homologues. As expected, a reduction in transition temperatures was observed when compared to the parent cinnamoyloxy derivatives. This homologous series of compounds exhibit a nematic, B_1 and B_2 phases.

The change in the position of fluorine in the middle phenyl ring from *ortho* to *meta* position (series **3.I** and **3.II**), does not affect the mesophase behaviour except for minor changes in the transition temperatures. The presence of fluorine at *meta* position, probably stabilizes a

columnar phase. For example, compound **3.B.9** shows a B_2 phase while compound **3.D.1** exhibits a columnar B_1 phase.

Surprisingly, the unsubstituted parent compound **3.E.1** does not show any mesophase and melts at 143°C while the corresponding fluorine substituted compounds namely, compounds **3.B.9** and **3.D.1** show direct transitions from N to B_2 and N to B_1 phases respectively. This is one of the best examples to show that although the parent compounds do not show any mesophase, the fluorine substituted compounds induce both N and B-phases (B_1 and B_2 phases).

Comparison between the mesophases of compounds of series 3.IV and 3.V:

These bent-core compounds are derived from resorcinol, containing a fluorine at *ortho* position on the middle phenyl ring and the arms are extended as cinnamates or α-methylcinnamates. The cinnamoyloxy derivatives exhibit B_6, B_1 and B_{X5} phases on ascending the homologous series (series **3.IV**). Interestingly, the compounds exhibiting B_{X5} phase which are derived from resorcinol show an antiferroelectric switching behaviour as compared to the naphthalene derivatives showing the B_{X3} mesophase which does not switch.
However, the compounds containing α-methylcinnamoyloxy groups are non-mesomorphic and the melting points, and their enthalpies are recorded in table **3.7**.

Comparison between the mesophases of compounds derived from 1,3-dihydroxybenzene and 2,7-dihydroxynaphthalene as the central units:

It is very clear from these investigations that the compounds derived from 2,7-dihydroxynaphthalene exhibit a nematic phase irrespective of the position of fluorine in the side wings for both cinnamates and α-methylcinnamates. Interestingly, the nematic phase gets stabilized even for n-tetradecyl chains without suppressing the B-phases. However, the corresponding symmetrical compounds which are derived from 1,3-dihydroxybenzene do not show a nematic phase even for shorter chains. In both the central cores one would expect the bending angle of about 120°. This is an indirect evidence that the compounds derived from 2,7-dihydroxynaphthalene as the central unit must be providing a bending angle of about $120< \theta < 140$, which is attributable to conformational changes in the arms. Hence the direct transitions from calamitic to B-phases are feasible. While the compounds derived from 1,3-dihydroxybenzene as the central unit might have a bending angle of about 120° and hence only the B-phases are expected. Since the nematic phase is not observed in the 1,3-

dihydroxybenzene derivatives, the induction of a nematic phase is not completely due to the flexible cinnamates, as well as due to the bending angle defined by the central core. In addition, the compounds containing α-methylcinnamoyloxy groups having 2,7-dihydroxynaphthalene as the central unit exhibit B-phases and a nematic phase while the corresponding 1,3-dihydroxybenzene analogues do not show any mesophase inspite of the fluorine substitution on the middle phenyl ring. From these observations one can infer that, 2,7-dihydroxynaphthalene appears to be a good angular central unit when compared with 1,3-dihydroxybenzene either to generate or to stabilize the mesophases and also to obtain rich polymesomorphism.

Experimental

2,7-Naphthylene bis(4-hydroxybenzoate), (3.1)

This was prepared as described in Chapter-2 (**2.21**)

2,7-Naphthylene bis(2-fluoro-4-hydroxybenzoate), (3.2)

This was prepared as described in Chapter-2 (**2.23**)

2,7-Naphthylene bis(3-fluoro-4-hydroxybenzoate), (3.3)

This was prepared as described in Chapter-2 (**2.25**)

1, 3-Phenylene bis(2-fluoro-4-benzyloxybenzoate), (3.4)

Resorcinol (1.1g, 10 mmol) and 2-fluoro-4-benzyloxybenzoic acid, (4.92g, 20 mmol) were dissolved in dry dichloromethane (50 ml). After the addition of N, N^{I} - dicyclohexylcarbodiimide (DCC), (4.5g, 22 mmol) and a catalytic amount of 4-(N, N - dimethylamino)pyridine (DMAP), the mixture was stirred at room temperature for about 15 hours. The dicyclohexylurea which precipitated was filtered off and washed with excess of chloroform (100 ml). The combined solution was washed with 2% aqueous acetic acid solution (3 × 50 ml) and 5% ice-cold aqueous sodium hydroxide solution (3 × 50 ml) and finally washed with water and dried over anhydrous sodium sulphate. The solid material obtained after removal of solvent was chromatographed on silica gel using chloroform as an eluent. Removal of solvent from the eluate afforded a white material which was crystallized from a mixture of chloroform and acetonitrile. Yield, 4.65g (82%); m.p. 161-162°C; ν_{max}(KBr): 2924, 2854, 1726, 1620, 1599, 1454, 1254, 1130 cm^{-1}; δ_H: 8.07-8.03 (t, 2H, ^{3}J8.6 Hz, Ar-H), 7.47-7.36 (m, 11H, Ar-H), 7.17-7.13 (m, 3H, Ar-H), 6.87-6.84 (dd, 2H, ^{3}J8.86 Hz, ^{4}J2.36 Hz, Ar-H), 6.79-6.76 (dd, 2H, ^{3}J12.66 Hz, ^{4}J2.36 Hz, Ar-H), 5.14 (s, 4H, 2 × $ArCH_2O$-).

1,3-Phenylene bis(2-fluoro-4-hydroxybenzoate), (3.5)

1,3-Phenylene bis (2-fluoro-4-benzyloxybenzoate) (4.5g) was dissolved in 1,4-dioxane (50 ml) and 5% Pd-C catalyst (1.0 g) was added. The mixture was stirred at 50°C in an atmosphere of hydrogen till the required quantity of hydrogen was absorbed. The resultant mixture was filtered hot and the solvent removed under reduced pressure. The solid material so obtained was passed through a column of silica gel and eluted with a mixture of 4% acetone in chloroform. Removal of solvent from the eluate gave a white material, which was

crystallized using a mixture of butan-2-one and petroleum-ether(b.p. 60-80°C). Yield, 2.8 g (91%); m.p. 270-272°C; ν_{max}: 3340, 1713, 1614, 1599, 1452, 1255, 1126 cm^{-1}; δ_H: 9.97(s, 2H, 2 × Ar–OH, exchangeable with D_2O), 8.17-8.13(t, 2H, ^{3}J8.68 Hz, Ar-H), 7.69-7.65(t, 1H, ^{3}J8.32Hz, Ar-H), 7.37-7.33(m, 3H, Ar-H), 6.99-6.96 (dd, 2H, ^{3}J8.74 Hz, ^{4}J2.28 Hz, Ar-H), 6.89-6.85(dd, 2H, ^{3}J12.82 Hz, ^{4}J2.32 Hz, Ar-H).

2,7-Naphthylene bis[4-(E-4-n-pentyloxycinnamoyloxy) 2-fluorobenzoate],(3.A.1)

A mixture of 2,7-naphthylene bis (2-fluoro-4-hydroxybenzoate)(200mg, 0.458 mmol), (E)-4-*n*-pentyloxycinnamic acid (215 mg, 0.917mmol), DMAP (11mg, 0.09 mmol) and dry chloroform(5 ml) was stirred for 10 minutes. To this mixture, DCC (208 mg, 1 mmol) was added and the stirring continued for 10 hours at room temperature. The precipitated N, N^1 - dicyclohexylurea was filtered off and washed with excess of chloroform (20 ml). Removal of solvent afforded a solid material which was purified by column chromatography on silica gel using 1% ethyl acetate in chloroform as an eluent. The white material obtained after removal of solvent from the eluate was crystallized using a mixture of chloroform and acetonitrile. Yield, 245 mg (62%); m.p. 175°C; ν_{max}: 2920, 2852, 1735, 1715, 1620, 1605, 1460, 1260, 1132 cm^{-1}; δ_H: 8.24-8.2(t, 2H, ^{3}J8.28 Hz, Ar-H), 7.95-7.93(d, 2H, ^{3}J8.88 Hz, Ar-H), 7.89-7.85(d, 2H, ^{3}J15.84 Hz, 2 × Ar-C<u>H</u>=CH-), 7.717-7.712(d, 2H, ^{4}J2.16 Hz, Ar-H), 7.56-7.54(d, 4H, ^{3}J8.76 Hz, Ar-H), 7.40-7.37(dd, 2H, ^{3}J8.86 Hz, ^{4}J2.2 Hz, Ar-H), 7.18-7.15(m, 4H, Ar-H), 6.95-6.93(d, 4H, ^{3}J8.76 Hz, Ar-H), 6.5-6.46(d, 2H, ^{3}J15.88 Hz, 2 × -CH=C<u>H</u>-COO-), 4.03-3.99(t, 4H, ^{3}J6.56 Hz, 2 × Ar-OCH_2-), 1.85-1.78(quin, 4H, ^{3}J6.64 Hz, 2 × Ar-OCH_2-<u>CH_2</u>-CH_2-), 1.48-1.37(m, 8H, 4 × -CH_2-<u>CH_2</u>-CH_2-), 0.96-0.93(t, 6H, ^{3}J7.12 Hz, 2 × -CH_2- <u>CH_3</u>).

2,7-Naphthylene bis[4-(E-4-n-hexyloxycinnamoyloxy) 2-fluorobenzoate], (3.A.2)

Yield, 64%; m.p. 148.5°C; ν_{max}: 2922, 2852, 1732, 1720, 1620, 1604, 1460, 1258, 1132 cm^{-1}; δ_H: 8.24-8.2(t, 2H, ^{3}J8.32 Hz, Ar-H), 7.95-7.93(d, 2H, ^{3}J8.92 Hz, Ar-H), 7.89-7.85(d, 2H, ^{3}J15.88 Hz, 2 × Ar-C<u>H</u>=CH-), 7.718-7.713(d, 2H, ^{4}J2.16 Hz, Ar-H), 7.56-7.54(d, 4H, ^{3}J8.76 Hz, Ar-H), 7.40-7.38(dd, 2H, ^{3}J8.86 Hz, ^{4}J2.2 Hz, Ar-H), 7.18-7.15(m, 4H, Ar-H), 6.95-6.93(d, 4H, ^{3}J8.72 Hz, Ar-H), 6.5-6.46(d, 2H, ^{3}J15.88 Hz, 2 × -CH=C<u>H</u>-COO-), 4.03-4.0(t, 4H, ^{3}J6.56 Hz, 2 × Ar-OCH_2-), 1.84-1.77(quin, 4H, ^{3}J6.68 Hz, 2 × Ar-OCH_2-<u>CH_2</u>-CH_2-), 1.49-1.44(m, 4H, 2 × -CH_2-<u>CH_2</u>-CH_2-), 1.37-1.33(m, 8H, 4 × -CH_2-<u>CH_2</u>-CH_2-),0.93-0.89(t, 6H, ^{3}J7.04 Hz, 2 × -CH_2- <u>CH_3</u>).

2,7-Naphthylene bis[4-(E-4-n-heptyloxycinnamoyloxy) 2-fluorobenzoate],(3.A.3)

Yield, 61%; m.p. 135.5°C; ν_{max}: 2924, 2852, 1740, 1724, 1621, 1605, 1460, 1258, 1132 cm^{-1}; δ_H: 8.24-8.2(t, 2H, ^{3}J8.24 Hz, Ar-H), 7.95-7.93(d, 2H, ^{3}J8.88 Hz, Ar-H), 7.89-7.85(d, 2H, ^{3}J15.88 Hz, 2 × Ar-C<u>H</u>=CH-), 7.718-7.712(d, 2H, ^{4}J2.08 Hz, Ar-H), 7.56-7.54(d, 4H, ^{3}J8.72 Hz, Ar-H), 7.40-7.38(dd, 2H, ^{3}J8.86 Hz, ^{4}J2.16 Hz, Ar-H), 7.18-7.15(m, 4H, Ar-H), 6.95-6.93(d, 4H, ^{3}J8.72 Hz, Ar-H), 6.5-6.46(d, 2H, ^{3}J15.88 Hz, 2 × -CH=C<u>H</u>-COO-), 4.03-4.0(t, 4H, ^{3}J6.56 Hz, 2 × Ar-OCH_2-), 1.84-1.77(quin, 4H, ^{3}J6.68 Hz, 2 × Ar-OCH_2-<u>CH_2</u>-CH_2-), 1.5-1.33(m, 16H, 8 × -CH_2-<u>CH_2</u>-CH_2-), 0.92-0.88(t, 6H, ^{3}J6.76 Hz, 2 × -CH_2- <u>CH_3</u>).

2,7-Naphthylene bis[4-(E-4-n-octyloxycinnamoyloxy) 2-fluorobenzoate], (3.A.4)

Yield, 65%; m.p. 136°C; ν_{max}: 2924, 2855, 1749, 1730, 1625, 1603, 1460, 1258, 1130 cm^{-1}; δ_H: 8.24-8.2(t, 2H, ^{3}J8.04 Hz, Ar-H), 7.95-7.93(d, 2H, ^{3}J8.92 Hz, Ar-H), 7.89-7.85(d, 2H, ^{3}J15.88 Hz, 2 × Ar-C<u>H</u>=CH-), 7.717-7.713(d, 2H, ^{4}J2.06 Hz, Ar-H), 7.56-7.54(d, 4H, ^{3}J8.52 Hz, Ar-H), 7.40-7.38(dd, 2H, ^{3}J8.8 Hz, ^{4}J2.10 Hz, Ar-H), 7.18-7.16(m, 4H, Ar-H), 6.95-6.93(d, 4H, ^{3}J8.44 Hz, Ar-H), 6.5-6.46(d, 2H, ^{3}J16.0 Hz, 2 × -CH=C<u>H</u>-COO-), 4.03-4.0(t, 4H, ^{3}J6.52 Hz, 2 × Ar-OCH_2-), 1.84-1.77(quin, 4H, ^{3}J6.56 Hz, 2 × Ar-OCH_2-<u>CH_2</u>-CH_2-), 1.48-1.29(m, 20H, 10 × -CH_2-<u>CH_2</u>-CH_2-), 0.90-0.87(t, 6H, ^{3}J6.56 Hz, 2 × -CH_2- <u>CH_3</u>).

2,7-Naphthylene bis[4-(E-4-n-nonyloxycinnamoyloxy) 2-fluorobenzoate], (3.A.5)

Yield, 62%; m.p. 124.5°C; ν_{max}: 2924, 2855, 1745, 1730, 1625, 1603, 1460, 1258, 1130 cm^{-1}; δ_H: 8.24-8.2(t, 2H, ^{3}J8.09 Hz, Ar-H), 7.95-7.93(d, 2H, ^{3}J8.92 Hz, Ar-H), 7.89-7.85(d, 2H, ^{3}J15.88 Hz, 2 × Ar-C<u>H</u>=CH-), 7.716-7.712(d, 2H, ^{4}J2.16 Hz, Ar-H), 7.56-7.54(d, 4H, ^{3}J8.54 Hz, Ar-H), 7.40-7.37(dd, 2H, ^{3}J8.84 Hz, ^{4}J2.13 Hz, Ar-H), 7.18-7.16(m, 4H, Ar-H), 6.95-6.93(d, 4H, ^{3}J8.40 Hz, Ar-H), 6.49-6.46(d, 2H, ^{3}J15.98 Hz, 2 × -CH=C<u>H</u>-COO-), 4.03-4.0(t, 4H, ^{3}J6.56 Hz, 2 × Ar-OCH_2-), 1.84-1.77(quin, 4H, ^{3}J6.56 Hz, 2 × Ar-OCH_2-<u>CH_2</u>-CH_2-), 1.49-1.29(m, 24H, 12 × -CH_2-<u>CH_2</u>-CH_2-), 0.90-0.87(t, 6H, ^{3}J6.56 Hz, 2 × -CH_2- <u>CH_3</u>).

2,7-Naphthylene bis[4-(E-4-n-decyloxycinnamoyloxy) 2-fluorobenzoate], (3.A.6)

Yield, 60%; m.p. 122°C; ν_{max}: 2922, 2853, 1742, 1720, 1626, 1603, 1460, 1257, 1128 cm^{-1}; δ_H: 8.25-8.20(t, 2H, ^{3}J8.11 Hz, Ar-H), 7.95-7.93(d, 2H, ^{3}J8.88 Hz, Ar-H), 7.89-7.86(d, 2H, ^{3}J15.90 Hz, 2 × Ar-C<u>H</u>=CH-), 7.717-7.713(d, 2H, ^{4}J2.10 Hz, Ar-H), 7.56-7.54(d, 4H, ^{3}J8.54 Hz, Ar-H), 7.40-7.37(dd, 2H, ^{3}J8.88 Hz, ^{4}J2.06 Hz, Ar-H), 7.17-7.16(m, 4H, Ar-H), 6.95-6.93(d, 4H, ^{3}J8.36 Hz, Ar-H), 6.49-6.46(d, 2H, ^{3}J15.9 Hz, 2 × -CH=C<u>H</u>-COO-), 4.03-4.0(t,

4H, ^{3}J6.51 Hz, 2 × Ar-OCH$_2$-), 1.84-1.77(quin, 4H, ^{3}J6.52 Hz, 2 × Ar-OCH$_2$-CH$_2$-CH$_2$-), 1.49-1.29(m, 28H, 14 × -CH$_2$-CH$_2$-CH$_2$-), 0.89-0.87(t, 6H, ^{3}J6.52 Hz, 2 × -CH$_2$- CH$_3$).

2,7-Naphthylene bis[4-(E-4-n-undecyloxycinnamoyloxy)2-fluorobenzoate],(3.A.7)

Yield, 64%; m.p. 126.5°C; ν_{max}: 2922, 2852, 1741, 1720, 1619, 1605, 1460, 1257, 1128 cm^{-1}; δ_H: 8.24-8.20(t, 2H, ^{3}J8.28 Hz, Ar-H), 7.95-7.93(d, 2H, ^{3}J8.92 Hz, Ar-H), 7.89-7.85(d, 2H, ^{3}J15.84 Hz, 2 × Ar-CH=CH-), 7.718-7.713(d, 2H, ^{4}J2.04 Hz, Ar-H), 7.56-7.54(d, 4H, ^{3}J8.72 Hz, Ar-H), 7.40-7.38(dd, 2H, ^{3}J8.84 Hz, ^{4}J2.12 Hz, Ar-H), 7.18-7.15(m, 4H, Ar-H), 6.95-6.93(d, 4H, ^{3}J8.68 Hz, Ar-H), 6.50-6.46(d, 2H, ^{3}J15.92 Hz, 2 × -CH=CH-COO-), 4.03-4.0(t, 4H, ^{3}J6.52 Hz, 2 × Ar-OCH$_2$-), 1.84-1.77(quin, 4H, ^{3}J6.56 Hz, 2 × Ar-OCH$_2$-CH$_2$-CH$_2$-), 1.47-1.27(m, 32H, 16 × -CH$_2$-CH$_2$-CH$_2$-), 0.90-0.87(t, 6H, ^{3}J6.56 Hz, 2 × -CH$_2$- CH$_3$).

2,7-Naphthylene bis[4-(E-4-n-dodecyloxycinnamoyloxy)2-fluorobenzoate],(3.A.8)

Yield, 63%; m.p. 126.5°C; ν_{max}: 2922, 2853, 1739, 1720, 1623, 1605, 1458, 1257, 1128 cm^{-1}; δ_H: 8.24-8.20(t, 2H, ^{3}J8.32 Hz, Ar-H), 7.95-7.93(d, 2H, ^{3}J8.92 Hz, Ar-H), 7.89-7.85(d, 2H, ^{3}J15.84 Hz, 2 × Ar-CH=CH-), 7.717-7.712(d, 2H, ^{4}J2.12 Hz, Ar-H), 7.56-7.54(d, 4H, ^{3}J8.76 Hz, Ar-H), 7.40-7.38(dd, 2H, ^{3}J8.84 Hz, ^{4}J2.2 Hz, Ar-H), 7.18-7.15(m, 4H, Ar-H), 6.95-6.93(d, 4H, ^{3}J8.76 Hz, Ar-H), 6.50-6.46(d, 2H, ^{3}J15.88 Hz, 2 × -CH=CH-COO-), 4.03-3.99(t, 4H, ^{3}J6.56 Hz, 2 × Ar-OCH$_2$-), 1.82-1.77(quin, 4H, ^{3}J6.92 Hz, 2 × Ar-OCH$_2$-CH$_2$-CH$_2$-), 1.53-1.27(m, 36H, 18 × -CH$_2$-CH$_2$-CH$_2$-), 0.90-0.87(t, 6H, ^{3}J6.6 Hz, 2 × -CH$_2$- CH$_3$).

2,7-Naphthylene bis[4-(E-4-n-tetradecyloxycinnamoyloxy)2-fluorobenzoate], (3.A.9)

Yield, 60%; m.p. 125°C; ν_{max}: 2922, 2853, 1735, 1720, 1631, 1608, 1458, 1257, 1132 cm^{-1}; δ_H: 8.24-8.20(t, 2H, ^{3}J8.28 Hz, Ar-H), 7.95-7.93(d, 2H, ^{3}J8.92 Hz, Ar-H), 7.89-7.85(d, 2H, ^{3}J15.84 Hz, 2 × Ar-CH=CH-), 7.717-7.712(d, 2H, ^{4}J2.12 Hz, Ar-H), 7.56-7.54(d, 4H, ^{3}J8.76 Hz, Ar-H), 7.40-7.38(dd, 2H, ^{3}J8.84 Hz, ^{4}J2.12 Hz, Ar-H), 7.18-7.15(m, 4H, Ar-H), 6.95-6.93(d, 4H, ^{3}J8.72 Hz, Ar-H), 6.50-6.46(d, 2H, ^{3}J15.88 Hz, 2 × -CH=CH-COO-), 4.03-3.99(t, 4H, ^{3}J6.56 Hz, 2 × Ar-OCH$_2$-), 1.84-1.77(quin, 4H, ^{3}J6.68 Hz, 2 × Ar-OCH$_2$-CH$_2$-CH$_2$-), 1.54-1.27(m, 44H, 22 × -CH$_2$-CH$_2$-CH$_2$-), 0.90-0.87(t, 6H, ^{3}J6.6 Hz, 2 × -CH$_2$- CH$_3$).

2,7-Naphthylene bis[4-(E-4-n-hexadecyloxycinnamoyloxy)2-fluorobenzoate], (3.A.10)

Yield, 63%; m.p. 121°C; ν_{max}: 2924, 2853, 1738, 1720, 1629, 1608, 1456, 1257, 1130 cm^{-1}; δ_H: 8.24-8.20(t, 2H, ^{3}J8.26 Hz, Ar-H), 7.95-7.93(d, 2H, ^{3}J8.90 Hz, Ar-H), 7.89-7.85(d, 2H, ^{3}J15.88 Hz, 2 × Ar-CH=CH-), 7.717-7.712(d, 2H, ^{4}J2.12 Hz, Ar-H), 7.56-7.54(d, 4H, ^{3}J8.70

Hz, Ar-H), 7.40-7.38(dd, 2H, ^{3}J8.88 Hz, ^{4}J2.10 Hz, Ar-H), 7.18-7.15(m, 4H, Ar-H), 6.95-6.93(d, 4H, ^{3}J8.72 Hz, Ar-H), 6.50-6.46(d, 2H, ^{3}J15.88 Hz, 2 × -CH=C<u>H</u>-COO-), 4.03-3.99(t, 4H, ^{3}J6.50 Hz, 2 × Ar-OCH$_2$-), 1.84-1.77(quin, 4H, ^{3}J6.68 Hz, 2 × Ar-OCH$_2$-<u>CH$_2$</u>-CH$_2$-), 1.54-1.27(m, 52H, 26 × -CH$_2$-<u>CH$_2$</u>-CH$_2$-), 0.90-0.87(t, 6H, ^{3}J6.6 Hz, 2 × -CH$_2$- <u>CH$_3$</u>).

2,7-Naphthylene bis[4-(E-4-n-octadecyloxycinnamoyloxy)2-fluorobenzoate], (3.A.11)

Yield, 64%; m.p. 118.5°C; ν_{max}: 2924, 2852, 1740, 1724, 1627, 1608, 1458, 1256, 1130 cm^{-1}; δ_H: 8.24-8.20(t, 2H, ^{3}J8.12 Hz, Ar-H), 7.95-7.93(d, 2H, ^{3}J8.92 Hz, Ar-H), 7.89-7.85(d, 2H, ^{3}J15.84 Hz, 2 × Ar-C<u>H</u>=CH-), 7.718-7.713(d, 2H, ^{4}J1.96 Hz, Ar-H), 7.56-7.54(d, 4H, ^{3}J8.68 Hz, Ar-H), 7.40-7.38(dd, 2H, ^{3}J8.82 Hz, ^{4}J2.08 Hz, Ar-H), 7.18-7.16(m, 4H, Ar-H), 6.95-6.93(d, 4H, ^{3}J8.64 Hz, Ar-H), 6.50-6.46(d, 2H, ^{3}J15.88 Hz, 2 × -CH=C<u>H</u>-COO-), 4.03-3.99(t, 4H, ^{3}J6.52 Hz, 2 × Ar-OCH$_2$-), 1.84-1.77(quin, 4H, ^{3}J6.64 Hz, 2 × Ar-OCH$_2$-<u>CH$_2$</u>-CH$_2$-), 1.50-1.26(m, 60H, 30 × -CH$_2$-<u>CH$_2$</u>-CH$_2$-), 0.90-0.86(t, 6H, ^{3}J6.64 Hz, 2 × -CH$_2$- <u>CH$_3$</u>).

2,7-Naphthylene bis[4-(E-4-n-butyloxy-α-methylcinnamoyloxy)2-fluorobenzoate], (3.B.1)

Yield, 66%; m.p. 143.5°C; ν_{max}: 2924, 2854, 1749, 1740, 1726, 1615, 1603, 1460, 1230, 1117 cm^{-1}; δ_H: 8.25-8.2(m, 2H, Ar-H), 7.96-7.93(d, 2H, ^{3}J8.88 Hz, Ar-H), 7.90(s, 2H, 2 × Ar-C<u>H</u>=C(CH$_3$)-), 7.72-7.71(d, 2H, ^{4}J2.08 Hz, Ar-H), 7.48-7.46(d, 4H, ^{3}J8.72 Hz, Ar-H), 7.41-7.38(dd, 2H, ^{3}J8.86 Hz, ^{4}J2.16 Hz, Ar-H), 7.18-7.14(m, 4H, Ar-H), 6.98-6.95(d, 4H, ^{3}J8.72 Hz, Ar-H), 4.03-3.99(t, 4H, ^{3}J6.56 Hz, 2 × Ar-OCH$_2$-), 2.277-2.274(d, 6H, ^{4}J1.12 Hz, 2 × -CH=C(C<u>H$_3$</u>)COO-, 1.85-1.78(quin, 4H, ^{3}J6.6 Hz, 2 × Ar-OCH$_2$-<u>CH$_2$</u>-CH$_2$-), 1.48-1.37(m, 4H, 2 × -CH$_2$-<u>CH$_2$</u>-CH$_2$-), 0.96-0.93(t, 6H, ^{3}J7.16 Hz, 2 × -CH$_2$- <u>CH$_3$</u>).

2,7-Naphthylene bis[4-(E-4-n-pentyloxy-α-methylcinnamoyloxy)2-fluorobenzoate], (3.B.2)

Yield, 67%; m.p. 133°C; ν_{max}: 2924, 2854, 1748, 1738, 1728, 1616, 1603, 1460, 1230, 1119 cm^{-1}; δ_H: 8.25-8.2(m, 2H, Ar-H), 7.96-7.93(d, 2H, ^{3}J8.88 Hz, Ar-H), 7.90(s, 2H, 2 × Ar-C<u>H</u>=C(CH$_3$)-), 7.72-7.71(d, 2H, ^{4}J2.08 Hz, Ar-H), 7.48-7.46(d, 4H, ^{3}J8.72 Hz, Ar-H), 7.41-7.38(dd, 2H, ^{3}J8.86 Hz, ^{4}J2.16 Hz, Ar-H), 7.18-7.14(m, 4H, Ar-H), 6.98-6.95(d, 4H, ^{3}J8.72 Hz, Ar-H), 4.03-3.99(t, 4H, ^{3}J6.56 Hz, 2 × Ar-OCH$_2$-), 2.277-2.274(d, 6H, ^{4}J1.12 Hz, 2 × -CH=C(C<u>H$_3$</u>)COO-, 1.85-1.78(quin, 4H, ^{3}J6.6 Hz, 2 × Ar-OCH$_2$-<u>CH$_2$</u>-CH$_2$-), 1.48-1.37(m, 8H, 4 × -CH$_2$-<u>CH$_2$</u>-CH$_2$-), 0.96-0.93(t, 6H, ^{3}J7.16 Hz, 2 × -CH$_2$- <u>CH$_3$</u>).

2,7-Naphthylene bis[4-(E-4-n-hexyloxy-α-methylcinnamoyloxy)2-fluorobenzoate], (3.B.3)

Yield, 69%; m.p. 128.5°C; ν_{max}: 2924, 2854, 1747, 1738, 1728, 1618, 1603, 1462, 1230, 1117 cm^{-1}; δ_H: 8.25-8.2(m, 2H, Ar-H), 7.96-7.93(d, 2H, ^{3}J8.92 Hz, Ar-H), 7.91(s, 2H, 2 × Ar-C<u>H</u>=C(CH_3)-), 7.72-7.71(d, 2H, ^{4}J2.16 Hz, Ar-H), 7.48-7.46(d, 4H, ^{3}J8.8 Hz, Ar-H), 7.41-7.38(dd, 2H, ^{3}J8.87 Hz, ^{4}J2.2 Hz, Ar-H), 7.18-7.14(m, 4H, Ar-H), 6.98-6.95(d, 4H, ^{3}J8.76 Hz, Ar-H), 4.03-3.99(t, 4H, ^{3}J6.56 Hz, 2 × Ar-O<u>CH_2</u>-), 2.277-2.274(d, 6H, ^{4}J1.12 Hz, 2 × -CH=C(C<u>H_3</u>)COO-, 1.85-1.78(quin, 4H, ^{3}J6.64 Hz, 2 × Ar-OCH_2-<u>CH_2</u>-CH_2-), 1.5-1.33(m, 12H, 6 × -CH_2-<u>CH_2</u>-CH_2-), 0.94-0.90(t, 6H, ^{3}J7.0 Hz, 2 × -CH_2- <u>CH_3</u>).

2,7-Naphthylene bis[4-(E-4-n-heptyloxy-α-methylcinnamoyloxy)2-fluorobenzoate], (3.B.4)

Yield, 72%; m.p. 133.5°C; ν_{max}: 2924, 2854, 1742, 1728, 1612, 1601, 1462, 1230, 1117 cm^{-1}; δ_H: 8.25-8.21(m, 2H, Ar-H), 7.96-7.93(d, 2H, ^{3}J8.92 Hz, Ar-H), 7.91(s, 2H, 2 × Ar-C<u>H</u>=C(CH_3)-), 7.72-7.71(d, 2H, ^{4}J2.08 Hz, Ar-H), 7.49-7.46(d, 4H, ^{3}J8.76 Hz, Ar-H), 7.41-7.38(dd, 2H, ^{3}J8.86 Hz, ^{4}J2.16 Hz, Ar-H), 7.18-7.14(m, 4H, Ar-H), 6.98-6.95(d, 4H, ^{3}J8.76 Hz, Ar-H), 4.03-4.0(t, 4H, ^{3}J6.56 Hz, 2 × Ar-OCH_2-), 2.278-2.275(d, 6H, ^{4}J0.92 Hz, 2 × -CH=C(C<u>H_3</u>)COO-, 1.85-1.78(quin, 4H, ^{3}J6.68 Hz, 2 × Ar-OCH_2-<u>CH_2</u>-CH_2-), 1.51-1.32(m, 16H, 8 × -CH_2-<u>CH_2</u>-CH_2-), 0.92-0.89(t, 6H, ^{3}J6.72 Hz, 2 × -CH_2- <u>CH_3</u>).

2,7-Naphthylene bis[4-(E-4-n-octyloxy-α-methylcinnamoyloxy)2-fluorobenzoate], (3.B.5)

Yield, 70%; m.p. 121.5°C; ν_{max}: 2924, 2852, 1738, 1725, 1612, 1600, 1460, 1230, 1117 cm^{-1}; δ_H: 8.25-8.21(m, 2H, Ar-H), 7.96-7.93(d, 2H, ^{3}J8.92 Hz, Ar-H), 7.91(s, 2H, 2 × Ar-C<u>H</u>=C(CH_3)-), 7.72-7.71(d, 2H, ^{4}J2.16 Hz, Ar-H), 7.49-7.46(d, 4H, ^{3}J8.8 Hz, Ar-H), 7.41-7.38(dd, 2H, ^{3}J8.86 Hz, ^{4}J2.2 Hz, Ar-H), 7.18-7.14(m, 4H, Ar-H), 6.98-6.95(d, 4H, ^{3}J8.8 Hz, Ar-H), 4.03-4.0(t, 4H, ^{3}J6.56 Hz, 2 × Ar-OCH_2-), 2.278-2.275(d, 6H, ^{4}J1.2 Hz, 2 × -CH=C(C<u>H_3</u>)COO-, 1.85-1.78(quin, 4H, ^{3}J6.68 Hz, 2 × Ar-OCH_2-<u>CH_2</u>-CH_2-), 1.50-1.30(m, 20H, 10 × -CH_2-<u>CH_2</u>-CH_2-), 0.91-0.88(t, 6H, ^{3}J6.6 Hz, 2 × -CH_2- <u>CH_3</u>).

2,7-Naphthylene bis[4-(E-4-n-nonyloxy-α-methylcinnamoyloxy)2-fluorobenzoate], (3.B.6)

Yield, 72%; m.p. 118°C; ν_{max}: 2922, 2852, 1740, 1725, 1615, 1600, 1460, 1230, 1117 cm^{-1}; δ_H: 8.25-8.21(m, 2H, Ar-H), 7.96-7.93(d, 2H, ^{3}J8.92 Hz, Ar-H), 7.91(s, 2H, 2 × Ar-C<u>H</u>=C(CH_3)-), 7.72-7.71(d, 2H, ^{4}J2.16 Hz, Ar-H), 7.49-7.46(d, 4H, ^{3}J8.36 Hz, Ar-H), 7.41-

7.39(d, 2H, ^{3}J8.8 Hz, Ar-H), 7.17-7.14(m, 4H, Ar-H), 6.98-6.96(d, 4H, ^{3}J8.32 Hz, Ar-H), 4.03-4.0(t, 4H, ^{3}J6.36 Hz, 2 × Ar-OCH_2-), 2.278-2.275(d, 6H, ^{4}J1.2 Hz, 2 × -CH=C($\underline{CH_3}$)-COO-, 1.85-1.78(quin, 4H, ^{3}J6.4 Hz, 2 × Ar-OCH_2-$\underline{CH_2}$-CH_2-), 1.47-1.30(m, 24H, 12 × -CH_2-$\underline{CH_2}$-CH_2-), 0.91-0.88(t, 6H, ^{3}J6.72 Hz, 2 × -CH_2-$\underline{CH_3}$).

2,7-Naphthylene bis[4-(E-4-n-decyloxy-α-methylcinnamoyloxy)2-fluorobenzoate], (3.B.7)

Yield, 73%; m.p. 116.5°C; ν_{max}: 2924, 2850, 1738, 1725, 1612, 1605, 1460, 1236, 1118 cm^{-1}; δ_H: 8.25-8.21(m, 2H, Ar-H), 7.96-7.93(d, 2H, ^{3}J8.92 Hz, Ar-H), 7.91(s, 2H, 2 × Ar-C$\underline{H}$=C(CH_3)-), 7.72-7.71(d, 2H, ^{4}J2.08 Hz, Ar-H), 7.49-7.46(d, 4H, ^{3}J8.76 Hz, Ar-H), 7.41-7.38(dd, 2H, ^{3}J8.84 Hz, ^{4}J2.12 Hz, Ar-H), 7.18-7.14(m, 4H, Ar-H), 6.98-6.95(d, 4H, ^{3}J8.72 Hz, Ar-H), 4.03-4.0(t, 4H, ^{3}J6.56 Hz, 2 × Ar-OCH_2-), 2.278-2.275(d, 6H, ^{4}J1.16 Hz, 2 × -CH=C(C$\underline{H_3}$)COO-, 1.85-1.78(quin, 4H, ^{3}J6.68 Hz, 2 × Ar-OCH_2-$\underline{CH_2}$-CH_2-), 1.50-1.28(m, 28H, 14 × -CH_2-$\underline{CH_2}$-CH_2-), 0.91-0.87(t, 6H, ^{3}J6.48 Hz, 2 × -CH_2- $\underline{CH_3}$).

2,7-Naphthylene bis[4-(E-4-n-undecyloxy-α-methylcinnamoyloxy)2-fluorobenzoate], (3.B.8)

Yield, 71%; m.p. 111.5°C; ν_{max}: 2924, 2850, 1738, 1722, 1610, 1605, 1468, 1236, 1118 cm^{-1}; δ_H: 8.25-8.21(m, 2H, Ar-H), 7.96-7.93(d, 2H, ^{3}J8.96 Hz, Ar-H), 7.91(s, 2H, 2 × Ar-C$\underline{H}$=C(CH_3)-), 7.72-7.71(d, 2H, ^{4}J2.16 Hz, Ar-H), 7.48-7.46(d, 4H, ^{3}J8.8 Hz, Ar-H), 7.41-7.38(dd, 2H, ^{3}J8.84 Hz, ^{4}J2.2 Hz, Ar-H), 7.18-7.14(m, 4H, Ar-H), 6.98-6.95(d, 4H, ^{3}J8.8 Hz, Ar-H), 4.03-4.0(t, 4H, ^{3}J6.52 Hz, 2 × Ar-OCH_2-), 2.277-2.274(d, 6H, ^{4}J1.2 Hz, 2 × -CH=C(C$\underline{H_3}$)COO-, 1.85-1.78(quin, 4H, ^{3}J6.72 Hz, 2 × Ar-OCH_2-$\underline{CH_2}$-CH_2-), 1.49-1.27(m, 32H, 16 × -CH_2-$\underline{CH_2}$-CH_2-), 0.90-0.87(t, 6H, ^{3}J6.6 Hz, 2 × -CH_2- $\underline{CH_3}$).

2,7-Naphthylene bis[4-(E-4-n-dodecyloxy-α-methylcinnamoyloxy)2-fluorobenzoate], (3.B.9)

Yield, 69%; m.p. 119.5°C; ν_{max}(KBr): 2910, 2850, 1740, 1720, 1612, 1605, 1458, 1230, 1120 cm^{-1}; δ_H: 8.25-8.20(m, 2H, Ar-H), 7.96-7.93(d, 2H, ^{3}J8.96 Hz, Ar-H), 7.91(s, 2H, 2 × Ar-C$\underline{H}$=C(CH_3)-), 7.72-7.71(d, 2H, ^{4}J1.88 Hz, Ar-H), 7.48-7.46(d, 4H, ^{3}J8.72 Hz, Ar-H), 7.41-7.38(dd, 2H, ^{3}J7.82 Hz, ^{4}J2.0 Hz, Ar-H), 7.17-7.14(m, 4H, Ar-H), 6.98-6.95(d, 4H, ^{3}J8.68 Hz, Ar-H), 4.03-4.0(t, 4H, ^{3}J6.56 Hz, 2 × Ar-OCH_2-), 2.277-2.274(d, 6H, ^{4}J1.2 Hz, 2 × -CH=C(C$\underline{H_3}$)COO-, 1.83-1.77(quin, 4H, ^{3}J7.04 Hz, 2 × Ar-OCH_2-$\underline{CH_2}$-CH_2-), 1.47-1.27(m, 36H, 18 × -CH_2-$\underline{CH_2}$-CH_2-), 0.90-0.87(t, 6H, ^{3}J6.6 Hz, 2 × -CH_2- $\underline{CH_3}$).

2,7-Naphthylene bis[4-(E-4-n-tridecyloxy-α-methylcinnamoyloxy)2-fluorobenzoate], (3.B.10)

Yield, 72%; m.p. 117.5°C; ν_{max}(KBr): 2910, 2850, 1740, 1720, 1612, 1605, 1458, 1250, 1120 cm^{-1}; δ_H: 8.25-8.20(m, 2H, Ar-H), 7.96-7.93(d, 2H, ^{3}J8.92 Hz, Ar-H), 7.91(s, 2H, 2 × Ar-C<u>H</u>=C(CH_3)-), 7.72-7.71(d, 2H, ^{4}J2.0 Hz, Ar-H), 7.48-7.46(d, 4H, ^{3}J8.76 Hz, Ar-H), 7.41-7.38(dd, 2H, ^{3}J7.82 Hz, ^{4}J2.08 Hz, Ar-H), 7.17-7.13(m, 4H, Ar-H), 6.98-6.95(d, 4H, ^{3}J8.68 Hz, Ar-H), 4.03-4.0(t, 4H, ^{3}J6.56 Hz, 2 × Ar-OCH_2-), 2.277-2.274(d, 6H, ^{4}J0.88 Hz, 2 × -CH=C(C<u>H</u>$_3$)COO-, 1.83-1.77(quin, 4H, ^{3}J6.68 Hz, 2 × Ar-OCH_2-<u>CH_2</u>-CH_2-), 1.48-1.26(m, 40H, 20 × -CH_2-<u>CH_2</u>-CH_2-), 0.90-0.87(t, 6H, ^{3}J6.64 Hz, 2 × -CH_2- <u>CH_3</u>).

2,7-Naphthylene bis[4-(E-4-n-tetradecyloxy-α-methylcinnamoyloxy)2-fluorobenzoate], (3.B.11)

Yield, 70%; m.p. 107°C; ν_{max}: 2912, 2850, 1740, 1716, 1612, 1601, 1458, 1260, 1130 cm^{-1}; δ_H: 8.25-8.20(m, 2H, Ar-H), 7.96-7.93(d, 2H, ^{3}J8.88 Hz, Ar-H), 7.91(s, 2H, 2 × Ar-C<u>H</u>=C(CH_3)-), 7.72-7.71(d, 2H, ^{4}J2.08 Hz, Ar-H), 7.48-7.46(d, 4H, ^{3}J8.8 Hz, Ar-H), 7.41-7.38(dd, 2H, ^{3}J8.84 Hz, ^{4}J2.12 Hz, Ar-H), 7.18-7.14(m, 4H, Ar-H), 6.97-6.95(d, 4H, ^{3}J8.76 Hz, Ar-H), 4.03-4.0(t, 4H, ^{3}J6.52 Hz, 2 × Ar-OCH_2-), 2.276-2.274(d, 6H, ^{4}J0.88 Hz, 2 × -CH=C(C<u>H</u>$_3$)COO-, 1.84-1.77(quin, 4H, ^{3}J6.64 Hz, 2 × Ar-OCH_2-<u>CH_2</u>-CH_2-), 1.48-1.26(m, 44H, 22 × -CH_2-<u>CH_2</u>-CH_2-), 0.90-0.87(t, 6H, ^{3}J6.6 Hz, 2 × -CH_2- <u>CH_3</u>).

2,7-Naphthylene bis[4-(E-4-n-hexadecyloxy-α-methylcinnamoyloxy)2-fluorobenzoate], (3.B.12)

Yield, 68%; m.p. 108°C; ν_{max}: 2920, 2850, 1755, 1744, 1722, 1615, 1601, 1463, 1260, 1130 cm^{-1}; δ_H: 8.25-8.20(m, 2H, Ar-H), 7.96-7.93(d, 2H, ^{3}J8.92 Hz, Ar-H), 7.91(s, 2H, 2 × Ar-C<u>H</u>=C(CH_3)-), 7.72-7.71(d, 2H, ^{4}J1.92 Hz, Ar-H), 7.48-7.46(d, 4H, ^{3}J8.76 Hz, Ar-H), 7.41-7.38(dd, 2H, ^{3}J8.8 Hz, ^{4}J2.04 Hz, Ar-H), 7.17-7.14(m, 4H, Ar-H), 6.97-6.95(d, 4H, ^{3}J8.76 Hz, Ar-H), 4.03-4.0(t, 4H, ^{3}J6.52 Hz, 2 × Ar-OCH_2-), 2.276-2.274(d, 6H, ^{4}J0.95 Hz, 2 × -CH=C(C<u>H</u>$_3$)COO-, 1.84-1.77(quin, 4H, ^{3}J6.68 Hz, 2 × Ar-OCH_2-<u>CH_2</u>-CH_2-), 1.5-1.26(m, 52H, 26 × -CH_2-<u>CH_2</u>-CH_2-), 0.90-0.86(t, 6H, ^{3}J6.48 Hz, 2 × -CH_2- <u>CH_3</u>).

2,7-Naphthylene bis[4-(E-4-n-octadecyloxy-α-methylcinnamoyloxy)2-fluorobenzoate], (3.B.13)

Yield, 65%; m.p. 109°C; ν_{max}: 2920, 2850, 1755, 1742, 1720, 1610, 1605, 1463, 1260, 1130 cm^{-1}; δ_H: 8.25-8.20(m, 2H, Ar-H), 7.96-7.93(d, 2H, ^{3}J8.92 Hz, Ar-H), 7.91(s, 2H, 2 × Ar-

C<u>H</u>=C(CH_3)-), 7.72-7.71(d, 2H, ^{4}J1.86 Hz, Ar-H), 7.48-7.46(d, 4H, ^{3}J8.52 Hz, Ar-H), 7.41-7.38(dd, 2H, ^{3}J8.8 Hz, ^{4}J2.04 Hz, Ar-H), 7.17-7.14(m, 4H, Ar-H), 6.97-6.95(d, 4H, ^{3}J8.4 Hz, Ar-H), 4.03-4.0(t, 4H, ^{3}J6.48 Hz, 2 × Ar-O<u>CH_2</u>-), 2.276-2.274(d, 6H, ^{4}J0.95 Hz, 2 × -CH=C(C<u>H_3</u>)COO-, 1.84-1.77(quin, 4H, ^{3}J6.52 Hz, 2 × Ar-OCH_2-<u>CH_2</u>-CH_2-), 1.48-1.21(m, 60H, 30 × -CH_2-<u>CH_2</u>-CH_2-), 0.89-0.86(t, 6H, ^{3}J6.52 Hz, 2 × -CH_2- <u>CH_3</u>).

2,7-Naphthylene bis[4-(E-4-n-tetradecyloxycinnamoyloxy)3-fluorobenzoate], (3.C.1)

Yield, 65%; m.p. 142°C; ν_{max}: 2924, 2850, 1735, 1720, 1618, 1602, 1460, 1257, 1130 cm^{-1}; δ_H: 8.1-8.06(m, 4H, Ar-H), 7.96-7.94(d, 2H, ^{3}J8.92 Hz, Ar-H), 7.92-7.88(d, 2H, ^{3}J15.88 Hz, 2 × Ar-C<u>H</u>=CH-), 7.699-7.694(d, 2H, ^{4}J2.12 Hz, Ar-H), 7.57-7.54(d, 4H, ^{3}J8.76 Hz, Ar-H), 7.43-7.36(m, 4H, Ar-H), 6.95-6.93(d, 4H, ^{3}J8.8 Hz, Ar-H), 6.55-6.50(d, 2H, ^{3}J15.88 Hz, 2 × -CH=C<u>H</u>-COO-), 4.03-3.99(t, 4H, ^{3}J6.52 Hz, 2 × Ar-OCH_2-), 1.84-1.77(quin, 4H, ^{3}J6.72 Hz, 2 × Ar-OCH_2-<u>CH_2</u>-CH_2-), 1.50-1.26(m, 44H, 22 × -CH_2-<u>CH_2</u>-CH_2-), 0.90-0.86(t, 6H, ^{3}J6.64 Hz, 2 × -CH_2- <u>CH_3</u>).

2,7-Naphthylene bis[4-(E-4-n-dodecyloxy-α-methylcinnamoyloxy)3-fluorobenzoate], (3.D.1)

Yield, 66%; m.p. 111°C; ν_{max}: 2920, 2850, 1740, 1720, 1612, 1605, 1458, 1260, 1130 cm^{-1}; δ_H: 8.11-8.07(m, 4H, Ar-H), 7.97-7.95(m, 4H, Ar-H), 7.7(d, 2H, ^{4}J1.16 Hz, Ar-H), 7.49-7.47(d, 4H, ^{3}J8.6 Hz, Ar-H), 7.43-7.37(m, 4H, Ar-H), 6.97-6.95(d, 4H, ^{3}J8.6 Hz, Ar-H), 4.03-4.0(t, 4H, ^{3}J6.52 Hz, 2 × Ar-OCH_2-), 2.297-2.294(d, 6H, ^{4}J1.1 Hz, 2 × -CH=C(C<u>H_3</u>)COO-, 1.84-1.77(quin, 4H, ^{3}J6.6 Hz, 2 × Ar-OCH_2-<u>CH_2</u>-CH_2-), 1.47-1.27(m, 36H, 18 × -CH_2-<u>CH_2</u>-CH_2-), 0.90-0.87(t, 6H, ^{3}J6.44 Hz, 2 × -CH_2- <u>CH_3</u>).

2,7-Naphthylene bis[4-(E-4-n-tridecyloxy-α-methylcinnamoyloxy)3-fluorobenzoate], (3.D.2)

Yield, 68%; m.p. 112°C; ν_{max}: 2920, 2851, 1745, 1730, 1620, 1605, 1462, 1260, 1132 cm^{-1}; δ_H: 8.11-8.07(m, 4H, Ar-H), 7.97-7.95(m, 4H, Ar-H), 7.7(d, 2H, ^{4}J2.12 Hz, Ar-H), 7.49-7.47(d, 4H, ^{3}J8.8 Hz, Ar-H), 7.43-7.37(m, 4H, Ar-H), 6.97-6.95(d, 4H, ^{3}J8.76 Hz, Ar-H), 4.03-4.0(t, 4H, ^{3}J6.52 Hz, 2 × Ar-OCH_2-), 2.295-2.293(d, 6H, ^{4}J1.12 Hz, 2 × -CH=C(C<u>H_3</u>)COO-, 1.84-1.77(quin, 4H, ^{3}J6.72 Hz, 2 × Ar-OCH_2-<u>CH_2</u>-CH_2-), 1.47-1.27(m, 40H, 20 × -CH_2-<u>CH_2</u>-CH_2-), 0.90-0.87(t, 6H, ^{3}J6.56 Hz, 2 × -CH_2- <u>CH_3</u>).

2,7-Naphthylene bis[4-(E-4-n-tetradecyloxy-α-methylcinnamoyloxy)3-fluorobenzoate], (3.D.3)

Yield, 63%; m.p. 102°C; ν_{max}: 2920, 2851, 1742, 1730, 1620, 1606, 1464, 1256, 1132 cm^{-1}; δ_H: 8.11-8.07(m, 4H, Ar-H), 7.97-7.95(m, 4H, Ar-H), 7.70-7.69(d, 2H, ^{4}J1.96 Hz, Ar-H), 7.49-7.47(d, 4H, ^{3}J8.72 Hz, Ar-H), 7.43-7.36(m, 4H, Ar-H), 6.97-6.95(d, 4H, ^{3}J8.72 Hz, Ar-H), 4.02-4.0(t, 4H, ^{3}J6.56 Hz, 2 × Ar-OCH_2-), 2.295-2.293(d, 6H, ^{4}J1.16 Hz, 2 × -CH=C($C\underline{H_3}$)COO-, 1.84-1.77(quin, 4H, ^{3}J6.44 Hz, 2 × Ar-OCH_2-$\underline{CH_2}$-CH_2-), 1.47-1.26(m, 44H, 22 × -CH_2-$\underline{CH_2}$-CH_2-), 0.89-0.86(t, 6H, ^{3}J6.6 Hz, 2 × -CH_2- $\underline{CH_3}$).

2,7-Naphthylene bis[4-(E-4-n-hexadecyloxy-α-methylcinnamoyloxy)3-fluorobenzoate], (3.D.4)

Yield, 61%; m.p. 107°C; ν_{max}: 2920, 2850, 1742, 1730, 1620, 1605, 1468, 1256, 1132 cm^{-1}; δ_H: 8.18-8.07(m, 4H, Ar-H), 7.97-7.95(m, 4H, Ar-H), 7.705-7.70(d, 2H, ^{4}J1.92 Hz, Ar-H), 7.49-7.47(d, 4H, ^{3}J8.72 Hz, Ar-H), 7.43-7.36(m, 4H, Ar-H), 6.97-6.95(d, 4H, ^{3}J8.76 Hz, Ar-H), 4.02-4.0(t, 4H, ^{3}J6.52 Hz, 2 × Ar-OCH_2-), 2.295-2.293(d, 6H, ^{4}J1.12 Hz, 2 × -CH=C($C\underline{H_3}$)COO-, 1.84-1.77(quin, 4H, ^{3}J6.92 Hz, 2 × Ar-OCH_2-$\underline{CH_2}$-CH_2), 1.47-1.26(m, 52H, 26 × -CH_2-$\underline{CH_2}$-CH_2-), 0.89-0.86(t, 6H, ^{3}J6.6 Hz, 2 × -CH_2- $\underline{CH_3}$).

2,7-Naphthylene bis[4-(E-4-n-dodecyloxy-α-methylcinnamoyloxy)benzoate], (3.E.1)

Yield, 70%; m.p. 143°C; ν_{max}:2920, 2850, 1740, 1725, 1615, 1605, 1456, 1230 cm^{-1}; δ_H: 8.33-8.31(m, 4H, Ar-H), 7.96-7.94(d, 2H, ^{3}J8.96 Hz, Ar-H), 7.92(s, 2H, 2 × Ar-C$\underline{H}$=$C(CH_3)$-), 7.70-7.69(d, 2H, ^{4}J2.12 Hz, Ar-H), 7.49-7.46(d, 4H, ^{3}J8.76 Hz, Ar-H), 7.4-7.34(m, 6H, Ar-H), 6.97-6.95(d, 4H, ^{3}J8.8 Hz, Ar-H), 4.03-3.99(t, 4H, ^{3}J6.56 Hz, 2 × Ar-OCH_2-), 2.287-2.284(d, 6H, ^{4}J1.12 Hz, 2 × -CH=C($C\underline{H_3}$)-COO-, 1.83-1.77(quin, 4H, ^{3}J6.96 Hz, 2 × Ar-OCH_2-$\underline{CH_2}$-CH_2-), 1.47-1.27(m, 36H, 18 × -CH_2-$\underline{CH_2}$-CH_2-), 0.90-0.87(t, 6H, ^{3}J6.64Hz, 2 × -CH_2- $\underline{CH_3}$).

1,3-Phenylene bis[4-(E-4-n-hexyloxycinnamoyloxy)2-fluorobenzoate], (3.F.1)

Yield, 64%; m.p. 137.5°C; ν_{max}: 2924, 2855, 1734, 1725, 1635, 1603, 1458, 1261, 1120 cm^{-1}; δ_H: 8.18-8.14(m, 2H, Ar-H), 7.89-7.84(d, 2H, ^{3}J15.84 Hz, 2 × Ar-C$\underline{H}$=CH), 7.55-7.47(m, 5H, Ar-H), 7.21-7.12(m, 7H, Ar-H), 6.95-6.92(d, 4H, ^{3}J8.72 Hz, Ar-H), 6.49-6.45(d, 2H, ^{3}J15.88 Hz, 2 × -CH=C$\underline{H}$-COO-), 4.03-3.99(t, 4H, ^{3}J6.52 Hz, 2 × Ar-OCH_2-), 1.84-1.77(quin, 4H, ^{3}J6.64 Hz, 2 × Ar-OCH_2-$\underline{CH_2}$-CH_2-), 1.49-1.43(m, 4H, 2 × -CH_2-$\underline{CH_2}$-CH_2-), 1.37-1.33(m, 8H, 4 × -CH_2-$\underline{CH_2}$-CH_2-), 0.93-0.89(t, 6H, ^{3}J6.96 Hz, 2 × -CH_2- $\underline{CH_3}$).

1,3-Phenylene bis[4-(E-4-n-decyloxycinnamoyloxy)2-fluorobenzoate], (3.F.2)

Yield, 63%; m.p. 111°C; ν_{max}: 2922, 2853, 1740, 1718, 1630, 1601, 1458, 1261, 1123 cm^{-1}; δ_H: 8.18-8.14(m, 2H, Ar-H), 7.88-7.84(d, 2H, ^{3}J15.84 Hz, 2 × Ar-C<u>H</u>=CH-), 7.55-7.47(m, 5H, Ar-H), 7.21-7.12(m, 7H, Ar-H), 6.95-6.92(d, 4H, ^{3}J8.72 Hz, Ar-H), 6.49-6.45(d, 2H, ^{3}J15.88 Hz, 2 × -CH=C<u>H</u>-COO-), 4.02-3.99(t, 4H, ^{3}J6.56 Hz, 2 × Ar-OCH_2-), 1.84-1.77(quin, 4H, ^{3}J6.64 Hz, 2 × Ar-OCH_2-<u>CH_2</u>-CH_2-), 1.48-1.27(m, 28H, 14 × -CH_2-<u>CH_2</u>-CH_2-), 0.90-0.87(t, 6H, ^{3}J6.56 Hz, 2 × -CH_2- <u>CH_3</u>).

1,3-Phenylene bis[4-(E-4-n-dodecyloxycinnamoyloxy)2-fluorobenzoate], (3.F.3)

Yield, 60%; m.p. 110.5°C; ν_{max}: 2922, 2853, 1740, 1718, 1625, 1601, 1458, 1260, 1123 cm^{-1}; δ_H: 8.18-8.14(m, 2H, Ar-H), 7.88-7.84(d, 2H, ^{3}J15.84 Hz, 2 × Ar-C<u>H</u>=CH), 7.55-7.47(m, 5H, Ar-H), 7.21-7.12(m, 7H, Ar-H), 6.95-6.92(d, 4H, ^{3}J8.76 Hz, Ar-H), 6.49-6.45(d, 2H, ^{3}J15.88 Hz, 2 × -CH=C<u>H</u>-COO-), 4.02-3.99(t, 4H, ^{3}J6.56 Hz, 2 × Ar-OCH_2-), 1.84-1.77(quin, 4H, ^{3}J6.72 Hz, 2 × Ar-OCH_2-<u>CH_2</u>-CH_2-), 1.46-1.26(m, 36H, 18 × -CH_2-<u>CH_2</u>-CH_2-), 0.89-0.86(t, 6H, ^{3}J6.6 Hz, 2 × -CH_2- <u>CH_3</u>).

1,3-Phenylene bis[4-(E-4-n-tetradecyloxycinnamoyloxy)2-fluorobenzoate], (3.F.4)

Yield, 62%; m.p. 114.5°C; ν_{max}: 2922, 2853, 1742, 1718, 1625, 1603, 1458, 1260, 1125 cm^{-1}; δ_H: 8.18-8.14(m, 2H, Ar-H), 7.88-7.84(d, 2H, ^{3}J15.84 Hz, 2 × Ar-C<u>H</u>=CH), 7.55-7.47(m, 5H, Ar-H), 7.21-7.12(m, 7H, Ar-H), 6.95-6.92(d, 4H, ^{3}J8.76 Hz, Ar-H), 6.49-6.45(d, 2H, ^{3}J15.9 Hz, 2 × -CH=C<u>H</u>-COO-), 4.02-3.99(t, 4H, ^{3}J6.56 Hz, 2 × Ar-OCH_2-), 1.84-1.77(quin, 4H, ^{3}J6.68 Hz, 2 × Ar-OCH_2-<u>CH_2</u>-CH_2-), 1.48-1.22(m, 44H, 22 × -CH_2-<u>CH_2</u>-CH_2-), 0.89-0.86(t, 6H, ^{3}J6.6 Hz, 2 × -CH_2- <u>CH_3</u>).

1,3-Phenylene bis[4-(E-4-n-hexadecyloxycinnamoyloxy)2-fluorobenzoate], (3.F.5)

Yield, 60%; m.p. 113.5°C; ν_{max}: 2922, 2854, 1742, 1718, 1625, 1601, 1458, 1260, 1125 cm^{-1}; δ_H: 8.18-8.14(m, 2H, Ar-H), 7.88-7.84(d, 2H, ^{3}J15.88 Hz, 2 × Ar-C<u>H</u>=CH), 7.55-7.47(m, 5H, Ar-H), 7.21-7.12(m, 7H, Ar-H), 6.95-6.92(d, 4H, ^{3}J8.76 Hz, Ar-H), 6.49-6.45(d, 2H, ^{3}J15.88 Hz, 2 × -CH=C<u>H</u>-COO-), 4.02-3.99(t, 4H, ^{3}J6.52 Hz, 2 × Ar-OCH_2-), 1.84-1.77(quin, 4H, ^{3}J6.68 Hz, 2 × Ar-OCH_2-<u>CH_2</u>-CH_2-), 1.48-1.22(m, 52H, 26 × -CH_2-<u>CH_2</u>-CH_2-), 0.89-0.86(t, 6H, ^{3}J6.6 Hz, 2 × -CH_2- <u>CH_3</u>).

1,3-Phenylene bis[4-(E-4-n-octadecyloxycinnamoyloxy)2-fluorobenzoate], (3.F.6)

Yield, 65%; m.p. 108°C; ν_{max}: 2924, 2852, 1738, 1720, 1625, 1605, 1456, 1260, 1130 cm^{-1}; δ_H: 8.18-8.14(m, 2H, Ar-H), 7.88-7.84(d, 2H, ^{3}J15.84 Hz, 2 × Ar-C<u>H</u>=CH-), 7.55-7.47(m, 5H, Ar-H), 7.21-7.12(m, 7H, Ar-H), 6.95-6.92(d, 4H, ^{3}J8.76 Hz, Ar-H), 6.49-6.45(d, 2H, ^{3}J15.84 Hz, 2 × -CH=C<u>H</u>-COO-), 4.02-3.99(t, 4H, ^{3}J6.56 Hz, 2 × Ar-OCH_2-), 1.84-1.77(quin, 4H, ^{3}J6.72 Hz, 2 × Ar-OCH_2-<u>CH_2</u>-CH_2-), 1.46-1.21(m, 60H, 30 × -CH_2-<u>CH_2</u>-CH_2-), 0.89-0.86(t, 6H, ^{3}J6.6 Hz, 2 × -CH_2- <u>CH_3</u>).

1, 3-Phenylene bis[4-(E-4-n-octyloxy-α-methylcinnamoyloxy)2-fluorobenzoate], (3.G.1)

Yield, 65%; m.p. 89°C; ν_{max}: 2924, 2855, 1751, 1728, 1620, 1605, 1458, 1236, 1134 cm^{-1}; δ_H: 8.19-8.15(m, 2H, Ar-H), 7.9(s, 2H, 2 × Ar-C<u>H</u>=C(CH_3)-), 7.51-7.46(m, 5H, Ar-H), 7.23-7.11(m, 7H, Ar-H), 6.97-6.95(d, 4H, ^{3}J8.76 Hz, Ar-H), 4.02-3.99(t, 4H, ^{3}J6.52 Hz, 2 × Ar-OCH_2-), 2.267-2.265(d, 6H, ^{4}J0.84 Hz, 2 × -CH=C(C<u>H_3</u>)-COO-, 1.84-1.77(quin, 4H, ^{3}J6.68 Hz, 2 × Ar-OCH_2-<u>CH_2</u>-CH_2-), 1.49-1.29(m, 20H, 10 × -CH_2-<u>CH_2</u>-CH_2-), 0.89-0.86(t, 6H, ^{3}J6.52 Hz, 2 × -CH_2- <u>CH_3</u>).

1, 3-Phenylene bis[4-(E-4-n-hexadecyloxy-α-methylcinnamoyloxy)2-fluorobenzoate], (3.G.2)

Yield, 61%; m.p. 96.5°C; ν_{max}: 2924, 2855, 1750, 1728, 1620, 1605, 1456, 1236, 1136 cm^{-1}; δ_H: 8.19-8.15(m, 2H, Ar-H), 7.9(s, 2H, 2 × Ar-C<u>H</u>=C(CH_3)-), 7.51-7.46(m, 5H, Ar-H), 7.23-7.11(m, 7H, Ar-H), 6.97-6.95(d, 4H, ^{3}J8.76 Hz, Ar-H), 4.02-3.99(t, 4H, ^{3}J6.52 Hz, 2 × Ar-OCH_2-), 2.267-2.265(d, 6H, ^{4}J1.04 Hz, 2 × -CH=C(C<u>H_3</u>)-COO-, 1.84-1.77(quin, 4H, ^{3}J6.64 Hz, 2 × Ar-OCH_2-<u>CH_2</u>-CH_2-), 1.46-1.26(m, 52H, 26 × -CH_2-<u>CH_2</u>-CH_2-), 0.89-0.86(t, 6H, ^{3}J6.52 Hz, 2 × -CH_2- <u>CH_3</u>).